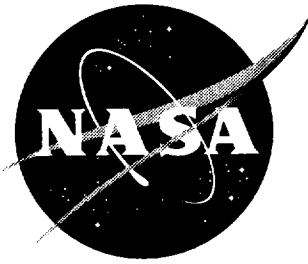


NASA/TM-1998-208440



Development of the Materials In Devices As Superconductors (MIDAS) Experiment

*R. M. Amundsen, J. C. Hickman, P. Hopson, Jr., E. H. Kist, Jr., J. M. Marlowe, E. Siman-Tov,
C. P. Turner, C. J. Tyler, J. E. Wells, S. A. Wise
Langley Research Center, Hampton, Virginia*

*R. Dickson
Computer Sciences Corporation, Hampton, Virginia*

*M. W. Hooker
Lockheed Martin Engineering and Sciences, Hampton, Virginia*

National Aeronautics and
Space Administration

Langley Research Center
Hampton, Virginia 23681-2199

May 1998

Available from the following:

NASA Center for AeroSpace Information (CASI)
7121 Standard Drive
Hanover, MD 21076-1320
(301) 621-0390

National Technical Information Service (NTIS)
5285 Port Royal Road
Springfield, VA 22161-2171
(703) 487-4650

TABLE OF CONTENTS

ABSTRACT.....	1
INTRODUCTION.....	1
INSTRUMENT DESCRIPTION	2
CARRIER HISTORY	5
EXPERIMENT DESIGN	7
HTS CIRCUIT BOARD DEVELOPMENT AND ASSEMBLY	7
HTS SUPPORT STAND DEVELOPMENT AND ASSEMBLY	8
CRYOCOOLER SELECTION AND MOUNTING DESIGN	10
ION PUMP SELECTION	13
ELECTRONICS BOX SELECTION AND DESIGN	14
VACUUM CHAMBER DESIGN	16
MINOR COMPONENT SELECTION AND DESIGN.....	17
SOFTWARE DESIGN.....	19
ANALYSIS	23
STRUCTURAL ANALYSIS	23
THERMAL ANALYSIS	28
ASSEMBLY	32
VACUUM CHAMBER ASSEMBLY	32
VACUUM CHAMBER PUMPDOWN.....	32
EXPERIMENT ASSEMBLY	35
TESTING	37
EMI/EMC TEST	38
THERMAL TEST	38
VIBRATION TEST	40
ACOUSTIC TEST.....	41
OFFGASSING TEST	41
OTHER TESTING	41
DOCUMENTATION	41
FLIGHT	42
POST-FLIGHT ACTIVITIES	47
SUMMARY OF DEVELOPMENT LESSONS LEARNED.....	49
CONCLUSIONS	51
ACKNOWLEDGMENTS	51
ADDITIONAL SOURCES.....	51
SYMBOLS.....	51
DEFINITIONS, ACRONYMS, ABBREVIATIONS	51
REFERENCES.....	52

FIGURES

FIGURE 1. MIDAS EXPERIMENT LAYOUT.....	3
FIGURE 2. HTS SAMPLE BOARD.....	3
FIGURE 3. FLIGHT CUBE AND SUPPORT STAND.....	9
FIGURE 4. CRYOCOOLER COMPRESSOR AND EXPANDER IN MOUNTING BRACKET.....	12
FIGURE 5. VACUUM CHAMBER ASSEMBLY.....	16
FIGURE 6. EXTERIOR HOUSING AND FRONT PANEL.....	18
FIGURE 7. SOFTWARE DEVELOPMENT PROCESS.....	22
FIGURE 8. EXPERIMENT STRUCTURAL FINITE ELEMENT MODEL.....	25
FIGURE 9. INTERIOR VIEW OF STRUCTURAL VACUUM CHAMBER MODEL.....	25
FIGURE 10. COPPER CUBE, EPOXY, & BOARDS DETAILED MODEL.....	26
FIGURE 11. EXPERIMENT MODE 3: 92 Hz.....	28
FIGURE 12. FAN PERFORMANCE VERSUS OUTLET AREA.....	29
FIGURE 13. EXPERIMENT THERMAL MODEL PREDICTION.....	30
FIGURE 14. HEAT LOAD DISTRIBUTION DURING COOLDOWN.....	30
FIGURE 15. PREDICTION VS. PERFORMANCE FOR COOLDOWN.....	31
FIGURE 16. OUTGASSING LOADS BY MATERIAL.....	33
FIGURE 17. PHOTOGRAPH OF FLIGHT HARDWARE WITH FINAL COVER, DURING OPERATION.....	35
FIGURE 18. PHOTOGRAPH OF INTERIOR OF ASSEMBLED EXPERIMENT.....	36
FIGURE 19. PHOTOGRAPH OF ASSEMBLED FLIGHT HARDWARE (VIEW OF FRONT PANEL).....	36
FIGURE 20. EMI TEST EXAMPLE SPECTRA: (A) ION PUMP ONLY, (B) ENTIRE EXPERIMENT ON.....	39
FIGURE 21. THERMAL TEST CYCLE.....	40
FIGURE 22. VIBRATION TEST SPECTRUM.....	40
FIGURE 23. CRYOCOOLER COLD FINGER TEMPERATURE DURING THE (A) FIRST AND (B) SECOND ON-ORBIT ITERATION OF THE MIDAS EXPERIMENT.....	43
FIGURE 24. ON-ORBIT RESISTANCE VERSUS TEMPERATURE DATA FOR THE THICK FILM SUPERCONDUCTORS ON CIRCUITS 1 (A) AND 3 (B).....	44
FIGURE 25. ON-ORBIT CURRENT DENSITY VS. VOLTAGE FOR SPECIMENS ON CIRCUITS 1 (A) AND 3 (B).....	45
FIGURE 26. COMPARISON OF PRE-FLIGHT AND ON-ORBIT J _c DATA FOR A TYPICAL THICK FILM SPECIMEN.....	46
FIGURE 27. COMPARISON OF ON-ORBIT I-V CHARACTERISTICS AT 124K DURING ITERATIONS 2 AND 3.....	46
FIGURE 28. EXAMPLE OF RESISTANCE VS. TEMPERATURE DATA FOR PRE-FLIGHT, FLIGHT, AND POST-FLIGHT.....	49

TABLES

TABLE 1. MIDAS COMPONENT MASSES.....	5
TABLE 2. COMPONENT DISSIPATED POWER.....	5
TABLE 3. CARRIER REQUIREMENTS FOR THE MIDAS EXPERIMENT.....	6
TABLE 4. CRYOCOOLER COMPARISON.....	11
TABLE 5. ION PUMP REQUIREMENTS.....	13
TABLE 6. ELECTRONICS BOX CIRCUIT CARDS.....	15
TABLE 7. PRIMARY STRUCTURE MARGIN-OF-SAFETY SUMMARY.....	27
TABLE 8. SUPERCONDUCTIVE TRANSITION TEMPERATURES FOR YBa ₂ Cu ₃ O _{7-x} THICK FILMS (PRE-FLIGHT, FLIGHT, AND POST-FLIGHT).....	48

Abstract

The Materials In Devices As Superconductors (MIDAS) spaceflight experiment was a NASA payload which launched in September 1996 on the Shuttle Atlantis (STS-79), was transferred to the Mir Space Station for several months of operation, and returned on STS-81. MIDAS was developed and built at NASA Langley Research Center (LaRC). The primary objective of the experiment was to determine the effects of microgravity and spaceflight on the electrical properties of high-temperature superconductive (HTS) materials. Cooling was provided by a small cryocooler, which maintained the specimens at or below 80 K. The superconductive specimens and the coldfinger of the cryocooler were mounted in a vacuum chamber, with vacuum levels maintained by an ion pump. The entire experiment was mounted for operation in a stowage locker inside Mir. The three separate cooling/warming cycles of the experiment were performed autonomously after circuit breaker activation by an astronaut. Each cycle consisted of approximately one day for cooldown, during which critical temperature data was gathered, 28 days below 80 K, during which critical current data was gathered, and one day for warm up, during which critical temperature data was again gathered. Data was stored on the experiment on solid state memory ("flash" cards), and downloaded after flight.

Issues discussed include some of the experiment historical background, such as several spacecraft that were to be the carrier at different times, the selection of components such as the cryocooler and ion pump, and the entire development through design, testing and flight. Flight data, in-flight anomalies and post-flight data reduction are also discussed. Some of the many challenges faced by project personnel were maintaining the HTS samples at cryogenic temperatures in a vacuum, preparation and bonding of the samples, meeting the mass and volume limits imposed by the Shuttle and Mir, and performing all necessary testing to meet required performance standards.

Introduction

The Materials In Devices As Superconductors (MIDAS) experiment was an autonomous locker-contained payload that was launched on the STS-79 mission of the Shuttle Atlantis and transported to the Priroda module on the Mir space station. After 90 days of operation, it was returned to Earth via the Shuttle. The primary objective of the experiment was to determine the effects of microgravity and spaceflight on the electrical properties of high-temperature superconductive (HTS) materials. These ceramic compounds exhibit unique characteristics that could enhance and improve space-borne scientific instruments^{1,2}. A secondary objective of the experiment was to use commercial off-the-shelf hardware where possible to evaluate component performance in a non-critical space payload.

The HTS materials used were $\text{YBa}_2\text{Cu}_3\text{O}_{7-x}$ and $\text{Bi}_2\text{Sr}_2\text{Ca}_2\text{Cu}_3\text{O}_x$, which have critical transition temperatures (i.e., the temperatures below which the materials are superconductive) of approximately 87 and 100K (for onset), respectively. The critical transition temperatures can vary somewhat depending on the sample purity and preparation technique. The experiment was designed to maintain the HTS samples below 80 K for three separate cycles of 28 days each. This thermal profile was designed to provide six separate measurements of the critical transition temperature (T_c), as well as continual measurement of the critical current density (J_c). The

critical current density is a measure of the maximum operating current per cross-sectional area that can be used with a given HTS material. Above the critical current density, the material is no longer superconductive and exhibits resistive behavior. The T_c and J_c properties determine the quality of superconductive materials; hence, these values can be used to determine degradation in specimens due to their operation in space.

The development of the experiment was technically challenging. The primary requirement to maintain the samples below 80 K was the driver for most of the technical complexity. This requirement involved keeping the samples under vacuum to eliminate air conduction, providing a radiation barrier, and limiting the thermal conduction of the structural supports and electrical connections. A small tactical cryocooler was used to provide cooling, and the heat generated by the cooler had to be dissipated to prevent damage to the compressor. Since the experiment was contained and operated in a locker, all heat from the experiment had to be controlled within the Mir and Shuttle requirements. Additional issues were: maintaining a vacuum in a sealed chamber within the limited mass, volume and power guidelines; design of the electronics and software to allow the experiment to be completely autonomous; use of low power components and electronics to avoid overheating; and completing all required testing and documentation within the schedule (including a change in launch vehicle).

There was about a six-year period from the inception of the project to completion of the flight mission. The concept was proposed in 1990, and the initial management review at Langley was held after three years of research and development on the materials. A Flight Request was submitted in January 1994. All reviews were held in accordance with the Langley guidelines for project reviews (LMI 7120.1). The Spaceflight Experiment Initiatives Review Committee (SEIRC) was convened in February 1994. The Preliminary Design Review (PDR) was held in August 1995, the Critical Design Review (CDR) in January 1996, and the Flight Readiness Review (FRR) in August in 1996. This meant that the majority of hardware development occurred between August 1995 and August 1996. The experiment was launched in September 1996, and returned from Mir in January 1997.

Instrument Description

The MIDAS experiment hardware consisted of the vacuum chamber with the HTS materials and their mechanical support, the tactical cryocooler and its control electronics, the data acquisition and control electronics, an ion pump, an ion pump back-up battery, a fan, and the mechanical support structure. MIDAS is shown in Figure 1 with the exterior foam and outer cover removed.

Central to the MIDAS experiment were the HTS samples, which were mounted on four thin ceramic substrate circuit boards isolated inside a vacuum chamber. Two boards were developed at LaRC, one board was supplied by a Russian co-investigator, and one was supplied by the Eaton Corporation. The LaRC boards consisted of $YBa_2Cu_3O_{7-x}$ superconductive elements deposited on a polycrystalline yttria-stabilized zirconia (YSZ) substrate via a screen-printing process. Each test circuit (or board) possessed six superconductive elements, which are the dark traces shown in Figure 2. The Russian board contained three $YBa_2Cu_3O_{7-x}$ films and three $Bi_2Sr_2Ca_2Cu_3O_x$ films deposited via sputtering onto a single crystal of zirconia. The Eaton board contained six films of $YBa_2Cu_3O_{7-x}$ doped with Pr, deposited by an ion-beam-assisted

deposition (IBAD) process onto lanthanum aluminate substrates. The boards are 2.5 x 2.5 cm and are mounted on the faces of a thermally conductive, hollow copper cube. Multiplexing and amplification of voltages measured from the superconductive elements and platinum resistance temperature devices were performed directly on the test circuit boards using multilayer thick film printing and active die-form multiplexers and amplifiers, resulting in active, microelectronic eight-channel hybrid superconductive/conventional circuits.

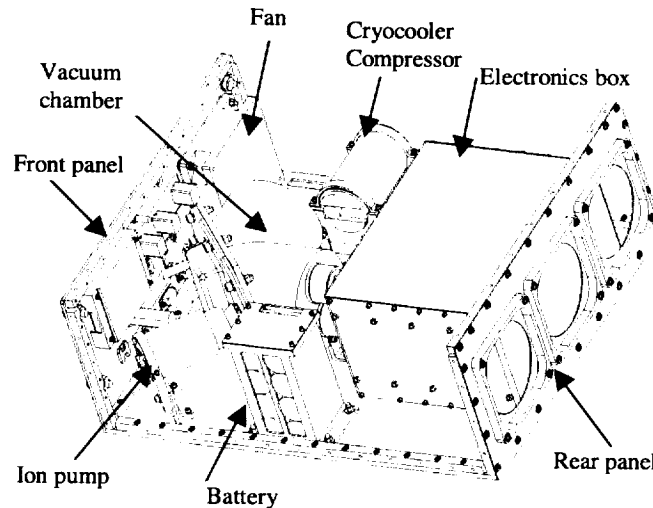


Figure 1. MIDAS experiment layout.

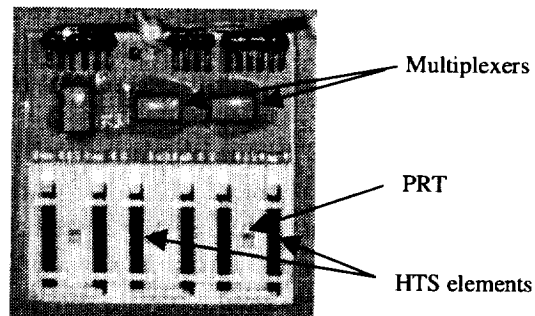


Figure 2. HTS sample board.

The substrates were bonded to the cube with a thin layer of epoxy. The cube could not be supported directly on the cryocooler expander (coldfinger) because this would place excessive loads on the expander during launch. Thus, a thermally isolating support stand was designed. The support stands were different on the flight and engineering model units due to outgassing concerns, as discussed later in the vacuum chamber design section. The engineering model was an epoxy resin / glass fiber cryogenic composite thin-walled tapered circular cone, and the flight stand was a four-legged stand of titanium alloy (Ti-6Al-4V). Both stands were designed to minimize the thermal conductance to the cube. The copper cube and titanium alloy support stand were both radiatively insulated using a multi-layer insulation (MLI) blanket.

The vacuum chamber was a stainless steel housing with an internal volume of approximately 1.5 liters. The chamber provided a vacuum to facilitate cooling the HTS samples; the maximum allowable pressure level was 10^{-3} torr, driven by having to limit air conduction. The cryocooler expander, ion pump, cube/stand assembly, and electrical connectors (to provide

exit for the HTS sample power and data lines) were mounted in the walls of the vacuum chamber. Once the chamber was pumped down after assembly, an ion pump mounted on the vacuum chamber via a mini-ConFlat-style flange maintained the vacuum. The ion pump was an integrated unit that consisted of the ion pump and control electronics. The ion pump had a pumping speed of 0.5 l/s at 10^{-5} to 10^{-8} torr, a maximum power usage of 1.25 watts over its operating range of 10 to 14 VDC, and was designed to operate for at least 9000 hours. The ion pump was powered via a DC-to-DC converter when the MIDAS experiment was powered externally and via a 12 VDC backup battery when the experiment was not externally powered.

The Texas Instruments tactical linear cryocooler was rated for 1 watt of cooling to 80K with an ambient temperature of 20°C. The cryocooler used 85 cc of helium in a sealed canister at a pressure of 250 psi as a working fluid and had a lifetime of approximately 4000 hours. The cryocooler compressor, which dissipated about 35 W, was attached to the experiment baseplate with aluminum brackets. The cryocooler expander, which dissipated about 15 W, was mounted to a face of the vacuum chamber via an O-ring sealed flange. The coldfinger extended from the expander into the vacuum chamber through an opening in the vacuum chamber wall. The cryocooler compressor and expander were connected via a narrow helium transfer line.

The remainder of the experiment included the electronics, the battery for backup operation of the ion pump, mechanical support assemblies and a fan in the front panel. The data acquisition and control electronics consisted of nine printed circuit boards in a ruggedized card cage. With the exception of three custom boards built by LaRC, all other boards were commercially provided. The fan was a small DC muffin fan that used a maximum of 3.4 W over its operating range of 24 to 56 VDC. The fan was attached to the MIDAS experiment front panel and provided approximately 65 cfm of airflow through the experiment housing.

The MIDAS experiment mass was approximately 24 kg. The mass and power for each component are shown in Table 1 and Table 2. Except for the fan, EMI filter and various switches (attached to the front panel), all experiment hardware was fastened to an aluminum baseplate. The experiment was contained within a 40 x 47 x 19 cm aluminum cover that was attached to the baseplate. A square fan intake port in the front panel was covered by a fine-mesh screen for cleanliness purposes. There were three fan exhaust holes in the rear panel of the housing which were covered by EMI screens. The exterior of the experiment was covered by closed-cell foam required by both Shuttle and Mir. Openings in the foam were provided for the front panel controls and fan screen intake and exhaust ports. The experiment mounted into either a Shuttle mid-deck locker or a Mir single-stowage locker by sliding into place and closing the locker front face – there were no hard mount points. This mounting configuration limited the thermal transfer out of the experiment via direct conduction and forced the heat exchange to depend primarily on efficient airflow. The foam also complicated the structural analyses since mechanical properties of the foam were not readily available and the stiffness and damping that the foam adds to the system are totally dependent on the packing. These factors made amplification in a vibration environment difficult to predict. On both Shuttle and Mir, power was provided via a cable connection to the front panel. The experiment was operated only on Mir; power on the Shuttle was provided for ion pump operation only, to maintain vacuum. Once on Mir, astronauts activated the experiment using circuit breakers on the front panel.

Table 1. MIDAS Component Masses

Assembly/Component		Weight (lb.)	Mass (kg)
Vacuum Chamber Assy		26.8	12.1
	Chamber	6.8	
	Cover	3.7	
	Cryocooler	3.6	
	Brackets	0.6	
	Hermetic connectors	0.5	
	Baseplate	7.7	
	Ion Pump	1.2	
	HTS Assembly	0.5	
	Pinch tube, misc. H/W	2.2	
Electronics box		10.6	4.8
Battery box		3.1	1.4
Cryocooler electronics assy		0.7	0.3
Front panel assy with wiring harness		6.3	2.8
Housing		5.7	2.6
Total (displayed values do not sum due to rounding)		53.1	24.1
Locker and foam		12.4	5.6
Total experiment mounted in locker		65.5	29.7

Table 2. Component Dissipated Power

Component	Maximum (W)	Typical (W)
Data Electronics	19	16
Cryocooler Compressor	35	17.5
Cryocooler Electronics	10	10
Cryocooler Expander	15	7.5
Fan	3	3
Ion Pump	3	1
Total Power	85	55

Carrier History

Initially, the MIDAS payload was designed to fly aboard the COMmercial Experiment Transporter (COMET) carrier, which was to launch on a Conestoga rocket. COMET consisted of two systems for housing experiments, the non-recoverable Service Module and the Recovery Module that separated from the flight vehicle after approximately 30 days in orbit and was recovered after re-entry. The MIDAS experiment requested a location on the recovery portion of COMET due to the desire for post-flight analysis of the test specimens. One advantage of COMET was the availability of a vacuum manifold, which would have allowed MIDAS to valve into the hard vacuum of space, rather than relying on internal vacuum pumping capability. MIDAS was slated for launch with the COMET-03 carrier, which was canceled due to lack of funding. Thus, in mid-1993, an alternative carrier was sought.

Several carriers were considered as possibilities, including COMET-02, Wakeshield and Get Away Special (GAS) on Shuttle, EURECA, and SmallSat. Inclusion as part of a student experiment on a Minuteman launch was also considered. At the time, the MIDAS carrier requirements were as shown in Table 3. The main difficulties were the desire for post-flight analysis and for more than seven days of operation in space, which would be difficult to achieve on a Shuttle flight. Operation in space for longer duration was desired, as the data would be used to predict survivability of HTS materials without degradation after many years of operation in space.

Table 3. Carrier Requirements for the MIDAS Experiment

Parameter	Requirements
Mission Duration	7 days minimum, desired to be as long as possible (COMET-03 was 28 days)
Environment Temperature	-20°C to 25°C
Voltage	Prefer 28 VDC
Pressure	13 to 16 psia atmosphere designed for; could tolerate vacuum with some redesign
Quasi-static Launch Load	12 g's designed for; could tolerate higher
Flight Vibration Level	11.5 g rms (+3 db for test) designed for; could tolerate higher
Nominal Orbit	No requirement on altitude or inclination
Late Access before Launch	No requirement on access before launch
Early Return after Landing	No requirement on access after landing
Microgravity Level:	
Continuous	Prefer less than 10^{-4} g, but not required
During Maneuvers	Prefer less than 10^{-1} g, but could tolerate higher
Telemetry	Prefer downlink, but not required. Current design for minimum of 1 downlink per 24 hours.

Participation in the Shuttle-Mir program offered an excellent flight opportunity for MIDAS, meeting the majority of the requirements without major redesign. The module suggested for MIDAS use was the Priroda module, a science module on Mir with standard 28V power available as well as several different types of experiment racks. Other US payloads were to be flown on Priroda, and the module was to be kept within documented specifications on humidity, temperature, oxygen level, etc³. Also, the Priroda design incorporated a vacuum vent manifold that would allow payloads access to space vacuum.

When MIDAS was manifested for operation on the Priroda module, the module had not yet been completed, launched and attached to Mir. As the date for Priroda launch approached, it became evident that, although a vacuum vent was designed into Priroda, it would not be implemented in the flight unit. At that point, MIDAS did not have any other system designed to provide vacuum, so the provision of a vacuum vent on the carrier was a key requirement. Thus, it was suggested that MIDAS operate aboard the Spektr module instead, which had an active vacuum vent system. However, Spektr was not designed for operation of US locker payloads;

there was no suitable power or mounting rack. Also, the environmental specifications were not as well defined. By this time, project personnel were actively working on an alternative design for MIDAS with an internal vacuum pump. Once the alternative design appeared feasible, the project personnel accepted the original payload slot on Priroda.

One of the challenging aspects of operating the payload on Priroda was the amount of required documentation. Since MIDAS was a payload on the Shuttle middeck for launch and return, the main Shuttle requirement document was that for middeck payloads⁴. In addition to the normal Shuttle documentation and safety reviews, there was another set of documents required for Priroda, referred to as the 100-series documents. These were ten documents, describing in great detail every facet of the experiment, operation, safety, etc., supplied electronically in blank-book form for the project to complete. Also, the NASA Johnson Space Center (JSC) personnel instituted a group called the SMART team, whose responsibility was to ensure that all Priroda payloads met operational standards equal to Shuttle standards, which required additional documentation.

The initial Mir documentation³ required five complete experiment assemblies for flight. This requirement was eventually relaxed, but some initial purchases were made using five complete units as a worst-case assumption. The final requirement was for one flight unit with spare parts available, an operational engineering model, and a mockup unit comprised of the non-metallic materials for offgassing testing. (Offgassing tests are performed to evaluate if hazardous materials are released during exposure to high temperatures in the manned Shuttle environment). The engineering model was developed to allow verification of the design and operation prior to assembly of the flight hardware.

Experiment Design

HTS Circuit Board Development and Assembly

The requirements on the HTS boards were to maintain them at 80K or below (75 K desired), to keep them isothermal, and to measure their temperatures within 0.5K accuracy. The HTS films were contained on thin substrates of yttria-stabilized-zirconia (YSZ) that were 2.5 x 2.5 cm. For the two LaRC-manufactured boards, the samples were deposited directly onto this main board, and the electronic components were contained on a 1.2 x 2.5 cm alumina board, which was bonded to one half of the larger board. Each entire board assembly was epoxied to one side of a hollow copper cube. The preparation of the HTS sample materials is discussed in depth in other project publications^{5,6}. The samples provided by Eaton Corporation used a similar configuration, but were deposited onto a 2.5 x 2.5 cm lanthanum aluminate single crystal substrate that was bonded to the 2.5 x 2.5 cm YSZ board. The samples provided by the Russian co-investigators were delivered on 1.2 x 1.2 cm boards, with only three HTS traces on each board. For these smaller boards, two were bonded to one half of the full-size YSZ board, and the electronics board was bonded to the other half.

Electrical connections were made using thin (0.0004-cm) gold wire bonds. The electronic die were encapsulated using epoxy, as were the gold wire bonds, to protect them from damage. The high thermal conductivity of the copper, epoxies, and alumina helped distribute the

heat from the active components, keeping the HTS samples isothermal. Copper foil was used for the thermal strap that attached the cube to the cryocooler coldfinger.

The electronic die components used for each board were two multiplexers and an amplifier. The amplifier was used to increase signal levels that were being measured remotely by the data acquisition electronics. The multiplexers were used to decrease the number of wires that needed to bridge the thermal gap from the vacuum chamber feedthrough connectors to the HTS sample circuit boards. The die were prescreened for operation at cryogenic temperatures. Although these components were not rated for operation at 75K, it was found that the components that operated at 75K did so reliably. Platinum resistance thermometers (PRTs) which had an accuracy of about 0.1K were used to make temperature measurements on the HTS boards. PRTs were placed between each pair of HTS samples, and one was also placed on the electronics board, to measure heating due to operation of the electronic components.

One important thermal issue was the bonding of the ceramic boards to the copper cube. This bond had to withstand multiple cycles from room temperature (or the 75°C cure temperature) to 75 K. Many epoxies were tested, and most proved too brittle, shattering the ceramic boards when they were cooled. Other requirements on the epoxy were that it be thermally conductive, both to facilitate spreading the heat from the active electronic devices on the boards, and to minimize the temperature differential between the coldfinger and the samples. Also, the epoxy had to have very low outgassing characteristics, to minimize both the outgassing load within the chamber and the contamination of the HTS materials. The EA9309 epoxy selected had a 75°C cure requirement to shorten the cure time, but even from this initial temperature it successfully withstood dozens of cycles to cryogenic temperature without excessive stress on the boards. One interesting discovery was that stress on the boards was intimately related to their exact mounting configuration. If the boards were mounted on the cube such that two edges were in contact, the shrinkage created by taking the assembly down to cryogenic temperatures caused the edges of the boards to push on each other and stressed the boards to failure at the edges. Testing the epoxy by bonding substrates to flat copper test pieces was not sufficient to ensure a successful bond. The bond used was kept to a thickness of roughly 0.005 cm by using small glass beads mixed into the epoxy. The thin bondline worked to minimize the volatiles released, minimize the thermal resistance, and mitigate the stresses produced.

HTS Support Stand Development and Assembly

The requirements on the support stand were that it structurally support the cube and samples through launch vibration and handling loads, outgas minimally in vacuum, and provide a minimal thermal path from the room temperature vacuum chamber to the cryogenic cube. The engineering model used a cryogenically compatible epoxy resin / glass fiber composite thin-walled tapered circular cone to support the cube. Two problems were encountered with this cone. First, the cone was found to continue to outgas, and was in danger of losing structural integrity due to the loss of resin, as well as producing a substantial vapor load. Secondly, since it was a solid piece, the MLI blanket used for radiation protection had to be placed under the foot of the cone. This required the use of two separate MLI blankets that were difficult to assemble in the limited vacuum chamber space and provided an excessive MLI surface area, slowing bakeout and pumpdown of the vacuum chamber.

In the flight design, the fiberglass support cone was eliminated and replaced with a four-legged titanium alloy (Ti-6Al-4V) stand, with each leg having a 1.2 x 1.2-mm square cross section. This alloy has low thermal conductivity, especially at cryogenic temperatures, and thus was thermally as effective as the fiberglass cone. The titanium plate under the cube used four raised pads at the mounting points to decrease the contact area and increase thermal resistance. The re-designed stand used for flight is shown in Figure 3. A thermal strap was used between the copper cube and the coldfinger to allow cooling of the HTS samples. This strap needed to provide maximum thermal transport without being a rigid structural element that would transmit loads from the cube to the coldfinger. Several designs were evaluated; the one actually used consisted of 11 strips of 0.1-mm thick copper foil. The strips were 2.5 cm wide by 7.6 cm long, and were press-mounted on both ends. The distance between the contact points at the coldfinger and cube was only 1 cm. In both ground testing and in flight, the strap performed well, resulting in a thermal gradient of about 2°C between the HTS samples and the coldfinger.

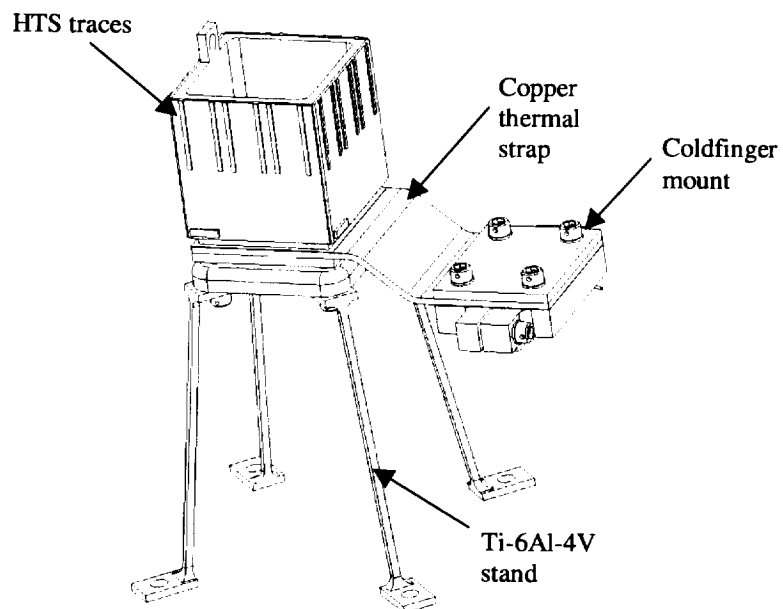


Figure 3. Flight cube and support stand.

A copper mounting block was used to attach the thermal strap to the coldfinger. Bolts were used to provide pressure around the circumference of the tip, and the block was also bonded to the tip with adhesive to ensure thermal conductivity. This method of attachment meant that once the cryocooler and mounting block were finally assembled, the cryocooler could not be removed, but it gave absolute confidence that the block would not lose contact with the coldfinger. All pressure mount points on the mounting block, thermal strap and copper cube were layered with Indium foil to decrease the thermal resistance of the joint.

The re-designed stand allowed an MLI blanket to be wrapped through the legs of the stand, around the cube, thermal strap, and coldfinger tip, yielding a smaller blanket. The blanket was again divided into two sections for ease of assembly. The blanket area was decreased by a factor of roughly five, and the number of layers was decreased from ten to five, for a total surface area improvement of 10:1 over the engineering model.

Cryocooler Selection and Mounting Design

Initially, a TRW miniature pulse-tube cooler was planned for use in the MIDAS experiment. This cooler met the lifetime and power requirements for MIDAS. By virtue of cooperative agreements between LaRC and TRW, it was to have been provided on loan to the MIDAS project for the duration of experiment testing and flight operation. However, due to the change in launch vehicles for MIDAS, and the resultant slip in launch dates, it was not feasible to accomplish this loan. Thus, in early 1995, MIDAS personnel evaluated commercial cryocoolers to select the optimum one for project specifications.

Initial criteria for cryocooler selection were that the cooler must be relatively inexpensive and available with a short lead time. "Tactical" coolers (i.e., originally designed for use on missiles) were found to satisfy both requirements. The initial survey found several potential cryocoolers, shown in Table 4, which were then further investigated for suitability. Although not a comprehensive list of cryocooler vendors, these coolers were determined to be appropriate candidates at that time. Another cryocooler that was investigated was the Sunpower cooler, which was undergoing testing at Goddard Space Flight Center (GSFC) at the time. It was felt, however, that the tight project schedule demanded a cooler that was already tested and ready for delivery. Thus, the decision was made to purchase a commercial cooler from the candidates listed in Table 4.

The cooler eventually selected for the MIDAS experiment was the Texas Instrument (TI) 1 W cooler. This cooler was selected because it met the mission requirement of 1 watt cooling at 80K while requiring a maximum power of 60 watts, having a robust input voltage range, tight temperature regulation, a relatively slow cool down time, low weight, low cost, and availability. The cooler consisted of three separate components (compressor, expander and electronics), which could be located as needed. A small-diameter transfer line connected the compressor and expander. As a linear cooler, it had slightly less generated noise than some of the other coolers, which were rotary in operation. The cooler compressor and expander, mounted in the flight support bracket and connected by the transfer line, are shown in Figure 4. The cooler was not available with a copper Con-Flat seal flange, so an O-ring seal was used where the expander mounted to the vacuum chamber. Four coolers were purchased, and all worked successfully. During ground testing the coolers outperformed expectations, generating cooldowns that were more rapid than predicted by analysis.

For the engineering model, the compressor was mounted in a support bracket that was not adjustable. The height of the bracket was determined by the required position of the expander where it mounted to the vacuum chamber, and by the geometry of the transfer line. The transfer lines were welded between the compressor and expander of each unit before they were shipped from the vendor. There was enough variability in the angle at which the line was welded that the line was put under stress when the compressor was mounted. For the engineering model, shims were used to reposition the mount. For the flight unit, the mount was re-designed so that it incorporated adjustability in two axes. When the cryocooler was mounted for flight, there was a slight twist in the transfer line that could not be completely accommodated by the bracket adjustability. After thorough testing, the transfer line was bent slightly to allow mounting of the cryocooler without stress in the line.

Table 4. Cryocooler Comparison

	Cincinnati Electronics - RICOR	Hughes	Magnavox	Texas Instruments
Model ⁸				
Cooling Capacity	K543	7050H-14	MX7055	1.0 Watt
Maximum Input Power	1 W @ 80K 35 W	1 W @ 80K 70 W	0.6 W @ 80K 50 W	1 W @ 80K 60 W
Input Voltage	18-24 VDC	17-32 VDC	17-32 VDC	17-32 VDC
Operating Temp. Regulation over Range (and at temperature)	-45 to 72°C ± 1K (0.5)	-50 to 70°C ± 3K (0.1)	-54 to 71°C ± 2K (0.5)	-54 to 71°C ± 1K (0.1)
Continuous Operation	best mode	ok	ok	maybe ²
Cool Down Time	5 min.	13 min.	10 min.	15 min.
Off/On Time	immediate	immediate ³ after 4K hrs.	immediate	immediate
Degradation			none (4K)	yes (to 0.55W)
Weight	2 lb.	4.2 lb.	2.5 lb.	4.0 lb.
Dimensions (cooler)	4.7" x 2.1" x 3.3"	4.7" x 2.5", 1.4" x 3.5" 2.5" x 2.5" x 1.0"	5.6" x 1.8", 1" x 2.7"	7.0 lb. 5.5" x 3", 2.2" x 3.5"
Dimensions (electronics)				
Leak Rate	0.8 x 10 ⁻⁷ scc/sec	10 ⁻⁷ scc/sec		10 ⁻⁷ scc/sec
Min. Vacuum	10 ⁻⁶ Torr	10 ⁻⁴ Torr (± x2)		10 ⁻⁶ Torr
Vibration/Shock		Meets 002, ⁴ except +X		MIL-STD-810E, method 514.4, procedure I ₆
EMI		incomplete meets 002 ⁴	"quiet"	
Cooler Noise		0.3 lb. (expander and compressor)	0.25 lb. (a.r)	<20dB@5m,2K ⁷ < 0.5 lb.
Cooler Vibration		4 months \$ 12,600 ¹	3 months \$ 17,500	6 months \$ 22,000
Lead Time	2 months			
Cost	\$ 10,000			

Table 4. Continued (Notes)

1. This price includes a pedestal to mount the cube on the cold finger
2. Their life cycle testing is done in 7-8 hour segments of on and off, no long-term continuous running
3. This conflicts with information presented to LaRC during a visit by Hughes personnel
4. Requirements in US/R-002, *Hardware General Design Standards and Test Requirements*, Korolev Rocket & Space Corporation Energia, December 1994.
5. After procurement of this cooler, during test, it was found that the cooler had enough margin to handle a 10^{-4} torr vacuum (possibly 10^{-3} torr) and still provide 75 K
6. After procurement of this cooler, during test, it was found that Shuttle and Mir EMI requirements were met with only the outer case for radiated emissions and with a filter for conducted emissions.
7. After procurement of this cooler, during test, it was found that noise level was insignificant in comparison to the fan used.
8. The following information applies to all the coolers listed:
 - The working fluid is helium.
 - The coolers with transfer lines require drawings that show the bends required for installation.
 - Temperature sensing is accomplished with a semiconductor device attached to the load, which means two additional lines from the cold tip area to the cooler electronics are required.
 - All the vendors (except Hughes) advise against mounting the cube on the cold finger.
 - None of the coolers listed are on the munitions list (per the individual vendors).

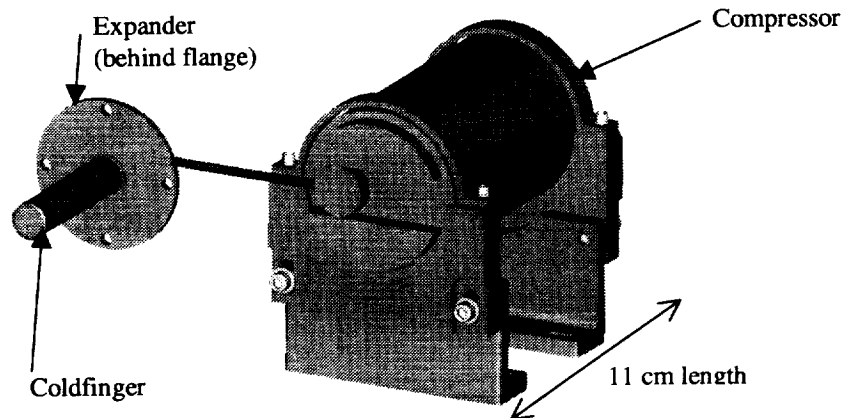


Figure 4. Cryocooler compressor and expander in mounting bracket.

The two main components of the cryocooler, the compressor and expander, needed to be kept near ambient temperature for efficient operation of the cryocooler. Their efficiencies decreased at higher temperatures -- the absolute upper limit for MIDAS was 86°C. The compressor was mounted using aluminum brackets, and placed directly in the path of the fan airflow. The expander generated less heat, but its temperature was more critical in determining the efficiency of operation of the cryocooler. The portion of the expander where the heat was dissipated was on the exterior of the vacuum chamber. Since this was a small part, the surface area needed to be increased to facilitate cooling. A finned flange was used on the outer diameter of the expander, and the expander was placed such that it was the first item in the line of the fan airflow, and thus received the coolest possible air. The flange was attached to the expander with epoxy, thus increasing the thermal transfer, but making it difficult to remove.

The cryocooler electronics consisted of a single card with a cable attaching it to 28 V DC, the cryocooler compressor, the ENABLE/DISABLE line, and the semi-conductor device (1N4148 diode) attached to the expander cold head. The box enclosing this card was designed

and built at LaRC. Adjustment of the cooler set-point (i.e., the temperature to which the coldfinger would cool during operation) was done by adjustment of a potentiometer (pot) on the cryocooler electronics. In testing on the engineering model, it was found that this pot needed to be accessed frequently. Thus, the design of the flight box was changed to allow easy access to this pot.

Ion Pump Selection

Due to changes in flight carriers and their specifications, the decision was not made until late in the program to include an ion pump as the sole method of maintaining the vacuum on MIDAS. Several vendors were evaluated based on qualifications for producing a space-quality pump on short notice. Five MODION ion pumps were purchased from Kernco, with specifications as shown in Table 5. Since the schedule time was critical, a full analysis of the vacuum load was not performed. Instead, the selection of the pump was based on a rough calculation of the leak rate through the O-ring seals and the outgassing from the chamber walls. In hindsight, a full vacuum load analysis should have been performed to determine the pumping speed requirement, including an analysis of outgassing from internal components and materials, leak rates from all seals, as well as a significant margin. This would have allowed selection of a pump with a robust performance margin, based on the best possible estimate of flight conditions.

Table 5. Ion Pump Requirements

Item	Requirement
Minimum Starting Pressure	1×10^{-4} torr
Minimum pumping speed of air	0.5 ℓ / s at 10^{-5} torr
Minimum Operational Life	9000 hours @ 10^{-6} torr or lower
Input Voltage	10 to 14 V DC
EMI/EMC	MSFC-SPEC-521
Maximum Power	1.25 W
Sealing Flange	Con-Flat

The pump selected had a flight history, and the vendor tested all units prior to delivery. However, one unit was tested after delivery at LaRC, both to gain experience with its operation and to ensure that it operated in accordance with the specifications. The pump was placed on a stainless steel vacuum tee, which was pumped to 10^{-8} torr. An ion gauge, calibrated to NIST-traceable standards, was attached to the tee to allow calibration of the ion pump monitor output. The volume of the tee, including all open volume such as the attached ion gauge, was roughly equal to the volume of the MIDAS vacuum chamber. The ion pump was started and allowed to run for a period of time to equilibrate. Then the section was valved off, and the ion pump was used to maintain the section under vacuum. In this test, it was discovered that the pump was extremely sensitive to pressure increases caused by water vapor. For example, when the pump was first activated the stainless steel section had not been thoroughly vacuum baked. It was very difficult to valve off the section and have the ion pump maintain the pressure level. Also, starting the ion gauge produced extreme variations in the ion pump voltage and current. The

activation of the hot-filament ion gauge vaporized water from the walls, which resulted in a sudden load on the pump. The tee was vacuum baked, with the ion pump running during all bakes as recommended by the vendor. After baking, the ion gauge could be ignited without disturbance to the ion pump, and the section could be valved off and held at 2×10^{-7} torr.

To unequivocally verify the capacity of the pump, it would have been desirable to test the pump on a volume with an exact known leak load. No calibrated leak units were easily available, so the pump was not tested in this manner. The pumping capacity of the pump was roughly verified by measuring the pressure rise rate on a volume that was then evacuated by the ion pump. Pressure rise rate was measured by valving off the volume and measuring the pressure rise using an ion gauge. Pressure rise rates as high as 1×10^{-7} torr-liter/sec (when the ion pump was off) were measured on the volume that the ion pump successfully maintained at vacuum. Pressure rise rates of exactly 5×10^{-6} torr-liter/sec (the pump specification) were not generated, so the maximum pump rate could not be verified.

The ion pump had a pressure monitor output with a voltage range of 0 to 5 V corresponding to 10^{-8} to 10^{-5} torr. In hindsight, it might have been better to have requested a range of 10^{-6} to 10^{-3} torr, which would have given more visibility into the system pressures. Since the chamber pressure was normally over 10^{-6} torr, the lower pressure range of the scale was superfluous. The monitor voltage was verified against calibrated ion gauge readings, and was found to be accurate.

Temperatures on the pump were measured during operation to ensure it did not exceed maximum operating temperatures, since the airflow in that area of the experiment would be low and the only direct thermal path was through the low conductivity stainless steel of the pump body and vacuum chamber. In that situation, even the 1 to 3 W dissipated by the pump could potentially be enough to warm the pump substantially. The pump did not usually draw more than 1 W and the temperature of the outer case did not rise by more than 2°C.

One interesting feature that was noted during testing was that the ion pump could "fold over" electronically when the pressure was above 10^{-5} torr. Normally, the monitor voltage increased with pressure up to 10^{-5} torr. When the pressure was above 10^{-5} torr, the monitor voltage would start decreasing, while the current used was increasing. When the pressure decreased again, the monitor voltage would rise up to 5 V and then start decreasing, with current readings decreasing throughout. Thus, the current level could be used as an indicator of whether the monitor voltage was "folded over," i.e., had gone above 5 V or 10^{-5} torr.

Electronics Box Selection and Design

Early in the project history, the decision was made by project personnel that the electronics for MIDAS would be purchased commercially, rather than custom designing and fabricating all the circuit boards and housing. This resulted in a substantial cost and time savings to the project. All the electronics boards used on MIDAS were purchased commercially, except for three that needed to be custom-made for specific project requirements. The card guides and rack that supported the cards structurally were commercial as well. The housing was fabricated at LaRC, because the commercial case exceeded mass guidelines. In-house fabrication of the

housing did not add substantially to the project cost since it was a relatively simple sheet metal case.

The boards used are listed in Table 6. All boards were staked (i.e., components lightly tacked with adhesive) using Hysol 608 epoxy. They were also conformal coated using Dow Corning (DC) 3140 RTV coating and DC 1204 primer. All internal ribbon cables that used PVC instead of Teflon insulation were also conformal coated, except a small video cable which was wrapped in Kapton tape. These coatings were necessary to allow the assembly to meet offgassing test requirements for payloads in habitable compartments on Shuttle and Mir.

Table 6. Electronics Box Circuit Cards

Component	Use	Vendor/Fabricator
Electronics box rack and card guides	Card support	ZiaTech
Backplane ZT-200	Circuit interfaces	ZiaTech
486 computer card	Microprocessor (main logic / control)	ZiaTech
PCMCIA card	Driver for Sundisks	ZiaTech
40 MB flash memory cards (Sundisks)	Data storage	Seagate
A/D converter card	Analog to digital conversions for data-taking	VersaLogic
Digital I/O card	Experiment control and timing	Winsystems
Power distribution card	Distribution of component power	LaRC
HTS power and mux interface card	Control HTS power and signals	LaRC
Digital I/O to HTS power and multiplexer card	Interface between these two cards	LaRC

Maximum power usage for the entire electronics box was approximately 19 W. The microprocessor chip itself used only 4 W. On the engineering model, a 386-microprocessor card was used, but this card was later upgraded to a 486 card with the same low power usage for the flight unit. Since the lithium battery for internal clock timing on the 486 card was not approved for flight, it was removed and a jumper soldered in its place. As a result the internal clock always restarted from the same date and time when the electronics box was powered. Thus, actual time had to be determined from external events. The microprocessor boards were purchased in several different shipments due to funding availability. Since the orders were placed at different times, the vendor had made certain changes to the boards; later ones were shipped with a different version of DOS, and with memory chips mounted in a different configuration. These differences had to be taken into account in writing the software and developing assembly procedures.

The electronics box housing was sheet metal and was not explicitly vented. This was the only closed-box component that would experience the potential change in pressure from the Shuttle pressure of 14.7 psi to the Priroda maximum of 18.8 psi. However, it was determined via a rough venting analysis that the small openings around each of the D-shell connectors in the

housing would provide more than enough flow area for the small potential pressure change. The housing included D-shell connectors for all power and signal lines, as well as for the keyboard, monitor and serial connections so that these could be run directly either from the electronics box or from the front panel. A serial connector was included so that software could be loaded onto the flash cards and data downloaded without opening the case. During assembly, it was found that some of the vendor-supplied boards contained cadmium-plated bolts, which were replaced since they are not suitable for spaceflight.

Vacuum Chamber Design

The vacuum chamber design went through many iterations due to changes in the operational parameters such as the availability of a vacuum manifold on the carrier, pump selection, size of the stowage locker, etc. The flight design of the vacuum chamber is shown in Figure 5. The final design included two flat end caps and a cover with flat sections, to allow enough room for all the components that were mounted in the chamber walls. These included two hermetic connectors, the cryocooler expander, ion pump, HTS cube/stand assembly, and pinch tube assembly. It was desired to have as many of the seals on the vacuum chamber as possible metal-to-metal, so ConFlat flanges with copper seals were used where possible. The ion pump was available on a mini-ConFlat flange with a copper gasket seal. However, the cryocooler was not available with a copper gasket seal, so a Viton O-ring was used. The hermetic connectors also came standard with O-rings, although their rated leak rates were very low (less than 10^{-9} cc He/sec). The cover was designed with an O-ring seal, because the shape of the cover would have been difficult to accommodate with a metal gasket, and use of a metal gasket would have made machining the cover more difficult. The pinch tube assembly was attached to the cover with a mini-ConFlat flange, using a copper gasket. One ConFlat flange was brazed to the cover, and one was brazed to a copper pinch tube, allowing a new pinch tube assembly to be easily attached to the chamber when necessary.

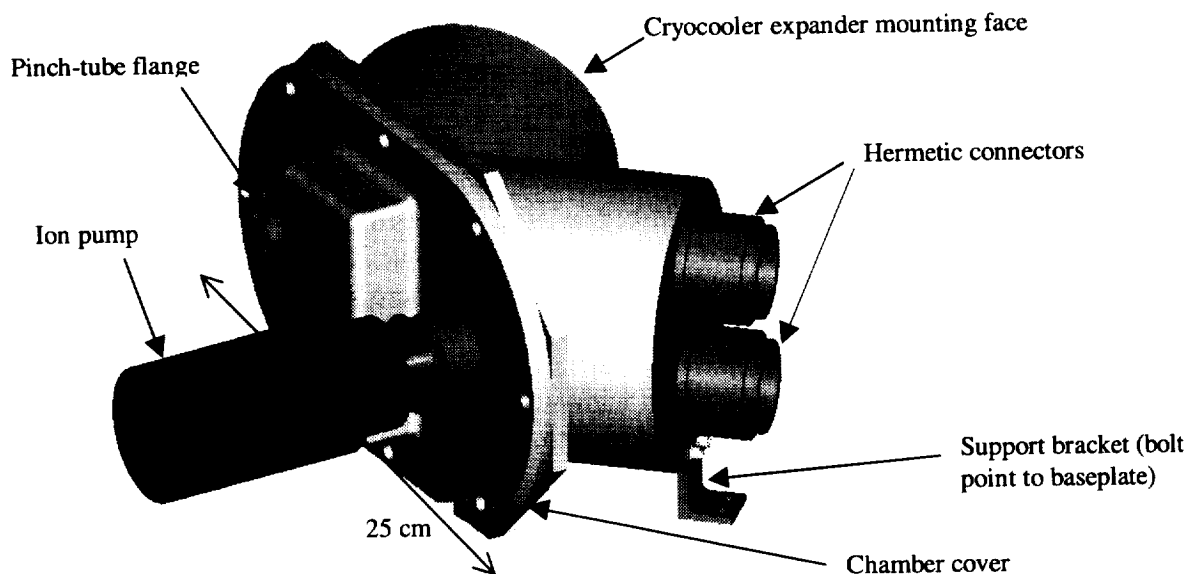


Figure 5. Vacuum chamber assembly.

A copper pinch tube was used for sealing the chamber instead of a valve, both for the level of vacuum seal it provided and because it posed no risks of opening or leaking during vibration. The copper was annealed before use, so that it would pinch off easily and smoothly. The pinch tube was 3/8" diameter and approximately 2.5 inches long, which allowed room for the pinch-off tool. The end of the pinch tube that remained on the pumping system after pinch-off could be used to determine whether the pinch leaked. All pinches performed were solid and did not leak. Originally, a part known as a "valve operator" was used on the engineering model chamber, which allowed removal of the valve part after closure. With this part, the chamber could be valved off, and then the valve removed from the chamber, leaving only a small stub fitting and the valve poppet. However, many problems were encountered in using the operator, and it was eventually removed from the design.

The chamber was designed of stainless steel to optimize the vacuum qualities. The two end cap portions were welded together, and the cover flange was welded on. This was done instead of hogging the whole part out of a solid piece to minimize the machining and material costs. The welds were extremely clean and uniform and did not present any leak or contamination problems.

The chamber was originally designed to mount entirely from the bottom of the baseplate. The baseplate was too thin to use bolt threads alone as a means of containment for the larger bolts, so a nut or other threaded material was required. Nuts could not be used on the underside of the baseplate since the underside had to be flat for mounting foam. Thus, the holes in the baseplate were counter-sunk from the underside, and a bolt was inserted into a threaded hole in the vacuum chamber. The chamber was attached at three points. After several design iterations, two of the mount points were modified to be small support brackets with two smaller bolts in each that could be installed from the top and have sufficient threaded length in the baseplate.

Minor Component Selection and Design

Minor components included the backup battery pack and components on the front panel. The batteries used on MIDAS were to provide a 12V source to power the ion pump during the times (such as transfer) when power was not available at the front panel. A relay was used to switch ion pump power from the front panel to the batteries when power at the front panel was interrupted. Eight Duracell standard D-cells wired in series provided the 12V battery power. The battery pack was originally supplied wrapped in polyvinylchloride (PVC). Project personnel were informed that this PVC would not be acceptable in the offgassing test, so it was changed over to a Teflon film wrapping. (Later, an examination of the Marshall Space Flight Center (MSFC) materials database revealed that the PVC would probably have been acceptable per MSFC-HDBK-527, since it was rated acceptable for offgassing, toxicity and flammability.) These batteries were the only non-metallic on the experiment that was not included as part of the offgassing test, since Duracell batteries of the same type had already undergone multiple successful offgassing tests.

The front panel is shown in Figure 6. Parts on the front panel included folding handles, circuit breakers, a two-color LED, a power connector, standard D-shell connectors for monitor, keyboard and serial GSE connections, a key mode switch, a fan and an EMI filter. The Amatom folding handles allowed the experiment to fit within the locker container with the handles folded

down, but they could be extended and locked in place when needed for transport. There were three circuit breakers on the front panel: MAIN, SYSTEM and BATTERY. When MAIN was activated, it allowed the 28V from the front panel to go to the electronics box, but only for conversion to 12V for use by the ion pump. Ion pump power supply integrity was verified by the front panel LED. This operating mode was implemented to maintain vacuum during transport and storage, when no other system power is provided. In the event of power failure, the front panel LED turned off and battery back-up power was automatically applied to the ion pump. The SYSTEM breaker applied 28V power to the entire experiment: the electronics box, cryocooler and fan. When the SYSTEM breaker was active, the front panel LED changed color. After the 486 computer booted up, the LED flashed continuously to indicate that the software was running properly. The BATTERY breaker was included as a safety cut-off. Normally, when no power was available at the front panel, the ion pump was powered from the backup battery. This breaker was available as a safety precaution to remove battery power from the ion pump. If this breaker were pulled, the ion pump could no longer use the 12V power from the battery.

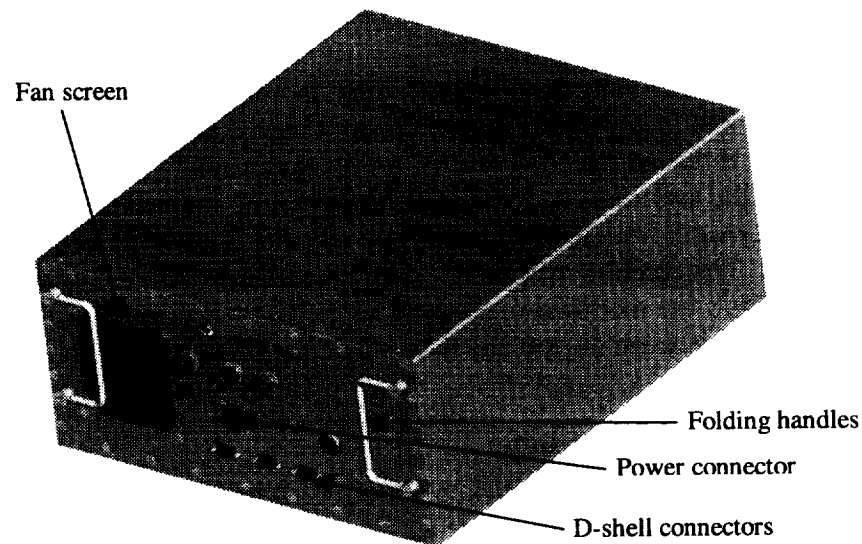


Figure 6. Exterior housing and front panel.

The front panel LED was originally designed as a single-color green LED. It would illuminate when system power was applied, and start flashing when the control program was initiated. A valuable suggestion was made by Kennedy Space Center (KSC) ground personnel during a safety review, that they would like to know when the front panel had power to it, so that they could know that their cable and power bus were working correctly. This was accomplished by changing the LED to a two-color Panasonic LED, which would be amber when there was power at the front panel, and green when the SYSTEM breaker was activated. It would still flash when the experiment was operating; the flashing was already implemented in software. This change, although simple for the experiment developers, was difficult to implement, because it was done at a time when all the 100-series integration documents with Priroda had already been written. Also, all the experiment segments for the Integrated Payload Requirements Document (IPRD) had already been developed, and the astronaut training was completed. The change was eventually allowed, benefiting ground operations at LaRC as well as at KSC.

The key mode switch was included to allow the experiment to be initiated autonomously in different modes. Three key positions were available. The flight software read the key position upon initialization and changed the experiment timing and sequence accordingly. In position 1, the experiment software would automatically start running the experiment in flight mode, which is the full three iteration, 90-day experiment. In position 2, the experiment software would automatically start in ground test mode (sometimes called a short-cycle test) which was used in various acceptance testing. The ground test mode ran for approximately 6 hours, which includes a cooldown cycle, two J_c measurements, and a warmup cycle. In position 3, the experiment software would start in data reduction mode and immediately end the program execution and return to the operating system prompt. This allowed for data retrieval or performing other functions, such as using the GSE software, without running the experiment automatically. The key was removed from the experiment before flight, so that the switch position could not be changed inadvertently while on-orbit. The key could only be removed from the switch in position 1, so that the experiment was guaranteed to be in flight mode when it was delivered on-orbit.

The fan selected for cooling the experiment was a small Comair DC muffin fan. Fan cooling had to be used since there was no forced air cooling provided by Priroda, and the foam on the exterior of the experiment severely curtailed any heat transfer by direct contact. It was a Priroda requirement to pull cooling air only from the front panel and exhaust it through the back. Extended discussion of the airflow requirements and fan selection is included in the thermal analysis section and in a MIDAS thermal analysis paper⁷.

An EMI filter was not originally part of the hardware design, because it was estimated (based on component specifications) that MIDAS would be able to meet the EMI requirements for Mir. However, based on initial EMI tests on the engineering model and also on tightened requirements from Mir, it was determined that EMI filtering would be required. This was more difficult to implement than expected, both because the EMI filter had to be matched to the internal power converter and because the filter needed to be the first item in the power line, directly after the circuit breaker. This meant that the filter had to be mounted to the front panel, where there was a limited amount of open area available. A small board was designed to hold the Interpoint EMI filter and associated components, and a cover box was designed that would protect it from particulates in the Priroda air. These were both mounted directly on the inside of the front panel, and successfully maintained the EMI at a level consistent with requirements.

Software Design

As mentioned in the electronics section, the target hardware for the software was mostly commercial off-the-shelf (COTS) which significantly simplified the software development for the project. The target hardware was MS-DOS compatible that allowed the use of a wide variety of proven COTS software development tools. The software development organization had experience, tools, and flight code from a previous project in the Ada programming language. Also, there was an effort in DoD and NASA to use Ada for mission critical software, therefore Ada was chosen as the programming language for the flight software. Documentation was based on NSDS-2100 and document templates were re-used from the CERES project. The software subsystem was used for a variety of pilot programs. One pilot program was for design and

development using Object Oriented Design and Programming (OOD & OOP). Another pilot was independent quality assurance activities.

In order to minimize the pilot programs' impact on the project, a separate, non-controlled (not conforming to pilot restrictions), prototype programming effort was started to support hardware development and other project development needs. The prototype code was written in C, using a public domain compiler and graphics package, in order to ensure independence from the flight code. This allowed the developer to learn about the hardware interface requirements in a natural way while supplying the hardware designers with insight into the design during development. Once the engineering model hardware had matured, the prototype software effort added an interface to precision lab instrumentation for verification of the data acquisition system. This prototype effort was eventually dubbed the Performance Measurement Verification System and was used as a validation of the flight software to precision instrumentation.

Design began with a requirements analysis using IBM's Scenarios method. While the method was useful in bringing the team together for discussions, it fell short in trying to define the autonomous system. By tying the scenarios to events occurring in the hardware system, the requirements became too closely linked to the target hardware and implementation. In order to have more abstraction from the hardware implementation, the requirements analysis method was switched to Colbert's Object Oriented Software Development (OOSD) method. The OOSD method allowed a better abstract model of the requirements and allowed the diagrams to be used as a design starting point. The requirement diagrams were placed and controlled in the process section of the software requirements document. The hardware I/O requirements were documented, in the interface section of the requirement's document, by describing each hardware device I/O registers and any timing and event sequence information. Finally, an attempt was made to track each requirement's traceability from the system requirements to the software requirements using a database. While this method looked promising, it faltered when the support personnel departed from LaRC and there was a lack of schedule and funding to assign new personnel to the task. Requirement traceability was maintained via the software requirements document, which was traceable to the systems requirements document.

Design continued with an architectural design. Originally, the architectural design began using Rumbaugh's Object Modeling Technique (OMT). This method seemed limited in the modeling of the state information of a multi-tasking system. Colbert's OOSD supported the use of Harrel's State Charts which does have notation for concurrence in the system. It turned out that OMT also supported Harrel's state notation, but that was not well documented in the text. Using the requirement diagrams as a starting point, the architectural design refined the diagrams by including a mapping of the requirements to the target hardware, yet leaving the design independent of the constructs of any particular programming language. At this point the pilot program had decided on another documentation standard, so the documentation of the design became more concentrated on the model diagrams and less on the other sections of the NSDS-2100 standard. The following diagrams were used extensively: 1) Object Interaction Diagrams (OID) which show a static view of the objects in the system and a representation of the interactions between the objects; and 2) Behavior Diagrams (BD) which show the dynamic view of an object. As an electronic analogy, the OID could be considered as a schematic, and the BD could be considered as the information given in an IC's databook. During this phase, a design workshop was held with all primary customers and team members on the science section of the

design. Another workshop was held with hardware personnel on the interface section of the design.

During the detailed design phase, the architectural diagrams (OIDs and BDs) were further refined. The next step in Colbert's OOSD method is to create language-dependent diagrams. In the case of Ada, the detailed design diagrams would be based on the Buhr notation for the structure charts. While the Buhr diagrams did not add any new design information and their value was questionable, they were generated anyway to test the code generation part of the computer aided software engineering (CASE) tool, which required the diagrams. The code generator produced the necessary packages and function calls that reflected the interfaces of the design. Next, Ada program design language (PDL) comments were added to the code structure to achieve traceability to the design. Finally, all the design code was compiled for type and visibility checking.

Coding went quite smoothly with only a couple of changes to the design needed to accommodate Ada and MS-DOS restrictions. Two code walkthroughs were held that covered all lines of flight software code. Not having the target hardware to test with, a logic analyzer was used to observe the I/O output patterns, while a function generator was used to provide inputs to the software system. The program was then tested on the target hardware and the results compared to the performance measurement verification system, the prototype software mentioned earlier, to give traceability to the calibrated instrumentation. All other testing came within the project's testing program and is described in later sections.

The data reduction software was produced in two phases. The purpose of the data reduction software is to convert the data into a raw representation as well as engineering units. First, a simple utility was created to convert the binary data into ASCII data. This software was developed in Ada and was able to reuse much of the flight software data routines to extract the data from the binary files. This allowed for quick conversion and checking of the data during the instrument tests. The second phase, producing the final data reduction software, was to convert the data into a format usable for analysis by the science team. The science and instrument team used several different machine types, so the final data reduction software needed to be cross-platform. This was achieved by using Microsoft's Excel product features. By creating an "add-in" for Excel, any Excel user would be able to convert and analyze the data. The add-in was created in the Visual Basic for Applications language. During the development of the final data reduction software, another needed utility was identified to split the data files into separate files for each board. This was necessary since the each HTS sample board contained different organizations' materials, some with proprietary requirements. This utility was also developed in Ada to reuse many of the data interface routines.

Once completed for baseline, the code was placed on drive P: of the target hardware, a 2-megabyte flash memory device. The final executable was 320 kilobytes, which was a 25% utilization of the available memory. The data was redundantly stored on four PCMCIA 20-megabyte flash disk devices with a 20% margin. There were 49 objects in the system and a total of about 3500 executable lines of code. While it does not encompass the whole story, Figure 7 shows the general process used to develop the MIDAS software.

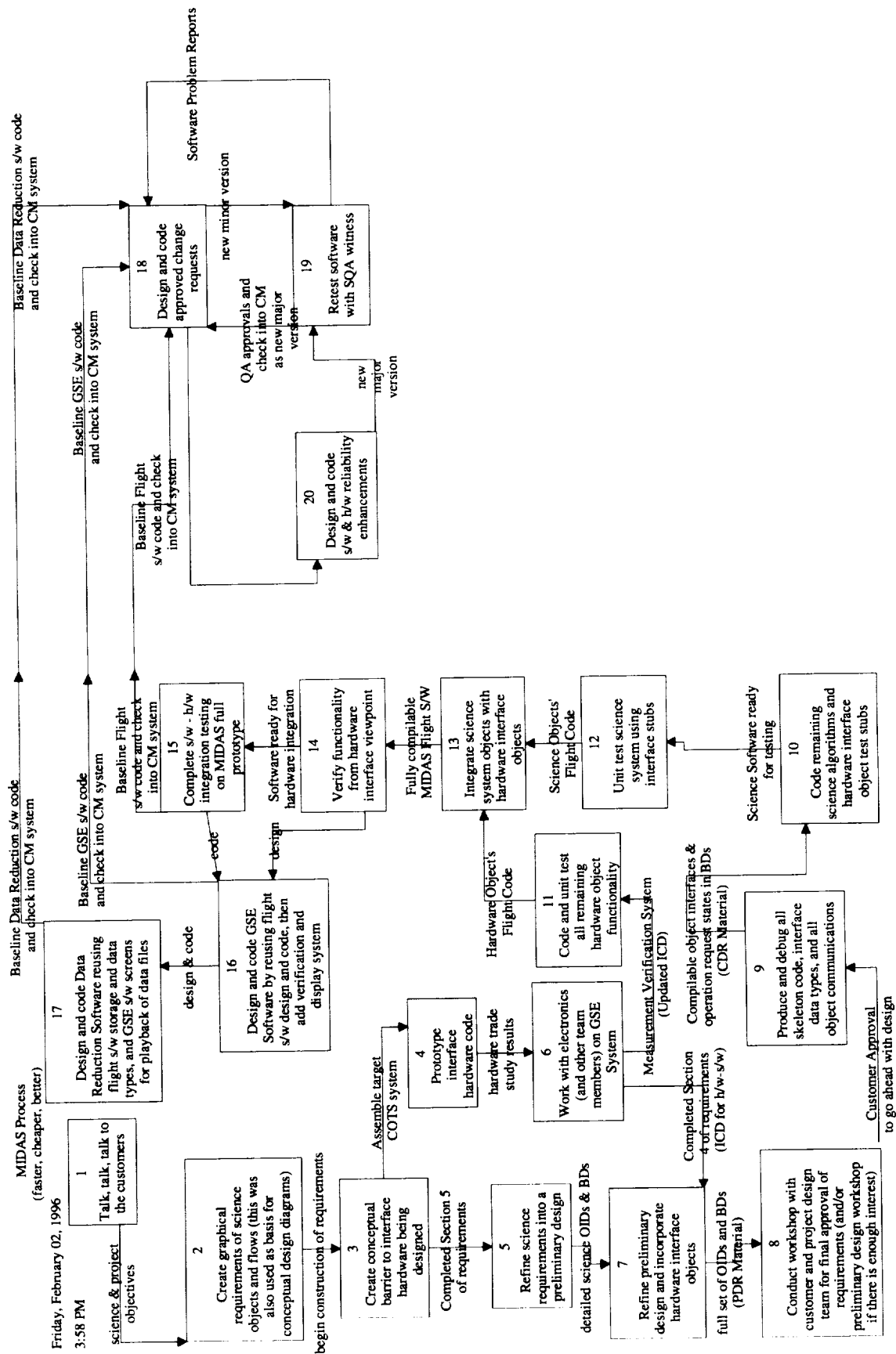


Figure 7. Software development process.

Analysis

Structural Analysis

Various structural analyses were performed in conjunction with vibration testing⁸ to verify that the MIDAS experiment met the safety criteria for operation in the Shuttle middeck and in the Priroda module on Mir. These analyses included:

1. static stress analysis of the entire experiment, including detailed assessment of fasteners, to verify MIDAS survival during shuttle launch/landing,
2. modal analysis of the entire experiment to verify that the natural modes of the MIDAS experiment encased in foam in the middeck locker would not couple with shuttle frequencies,
3. buckling analysis of the MIDAS vacuum chamber to ensure that the chamber would be safe under internal pressure loading,
4. buckling analysis of the MIDAS sample support stand (titanium spider) to ensure that the long, thin legs on the support stand were safe under all environments,
5. frequency response analysis, which was used to investigate whether the cyclic loading from the cryocooler compressor adversely affected the thin titanium tube that connects the compressor and cold tip, and
6. detailed static stress analysis of the copper cube, bonds, and boards to predict deflections and thermal stresses under cryogenic temperatures.

Since the MIDAS experiment required substantial structural and thermal analysis to verify the hardware for flight, the analysis team decided to create a single analysis math model that could be used by both structural and thermal analysts by using, as much as was practical, the CAD geometry files produced by the design engineers. The advantages of this concurrent engineering approach were that only one person needed to work the substantial task of actually developing this detailed model, geometry was only created once by the design engineer and was reused by the analysts which saved time and improved accuracy, only one model needed to be modified in the event that the design changed which vastly improved turn-around time, and thermal results could be readily evaluated by the structural analyst since the analysts were using a common model.

In implementing the shared math model, the analysts met prior to model development to discuss requirements, including which hardware components needed to be modeled, preferences for mesh densities and mesh characteristics, methods of modeling interfaces, and other modeling issues. On the structural analysis tasks specifically, MSC/NASTRAN was the primary finite element solver, and MSC/PATRAN was used to visualize static and animated results. On selected small tasks during the development process, Pro/Mechanica was used to evaluate specific components for specific structural issues; Pro/Mechanica was not selected as the solver for the shared analysis model since it did not (at that time) have an adequate thermal solver.

The final version of the structural finite element model of the full MIDAS experiment is shown in Figure 8. The features of this model important to the structural analyst are:

- The isolating foam, which surrounded the MIDAS experiment baseplate and cover, was included in the model solely for examining MIDAS' modal characteristics. Exact

mechanical properties of the L200FR isolating foam were unavailable; however, research on the mechanical properties of other foams showed that the Young's modulus could potentially range from 10 psi to 390 ksi. Modal analyses using this range of Young's moduli predicted that frequency results would vary by only ~25% over this very large range of foam stiffnesses. Reference 4 requires that the isolating foam have a stiffness equivalent to a spring rate of 22,000 lb/in or less, which is equivalent to a Young's modulus of ~71 psi for the MIDAS configuration. Since this value falls within the range of Young's moduli found for other foams, 71 psi was used in the model for the frequency calculations.

- The batteries, fan, cryocooler and ion pump were included in the model as non-structural masses, and were either modeled as solid elements with densities corresponding to component masses or as concentrated masses. The vendor verified structural adequacy of these components, and they were included in the model to capture their influence on the stress state of the experiment baseplate and on the experiment modal characteristics.
- The electronics box assembly was modeled in some detail as it was designed and built at Langley. The body, card guide panels, front panel, and mounting brackets were all modeled using plate elements for both stress and modal assessment, and fasteners were modeled with rigid elements for easy force recovery. The nine cards, card guides, connectors and backplane were modeled to accurately represent stiffnesses, masses and load paths only.
- Mounting brackets for the cryocooler compressor were accurately modeled using a combination of solid and rigid elements for stress and/or force recovery.
- The vacuum chamber assembly and mounting bracketry and fasteners were modeled in considerable detail using plate and rigid elements for inclusion in stress, buckling and modal analyses. Inside the chamber, shown in Figure 9, the sample support structure including titanium spider, fasteners, copper thermal strap, and copper cube were modeled using beam, plate, and rigid element meshes suitable for stress/force recovery.
- Most fasteners in the experiment were modeled using rigid elements to facilitate force recovery. The forces from the finite element model were then used in the appropriate equations⁹ to calculate margins of safety.

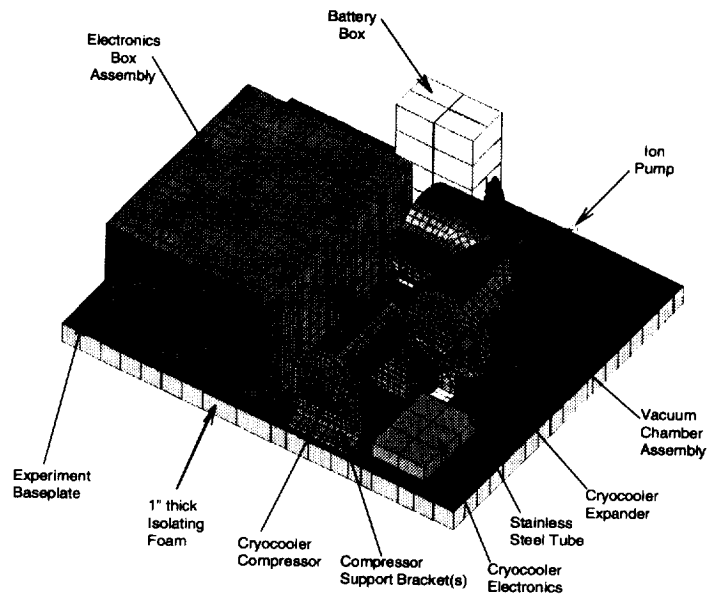


Figure 8. Experiment structural finite element model.

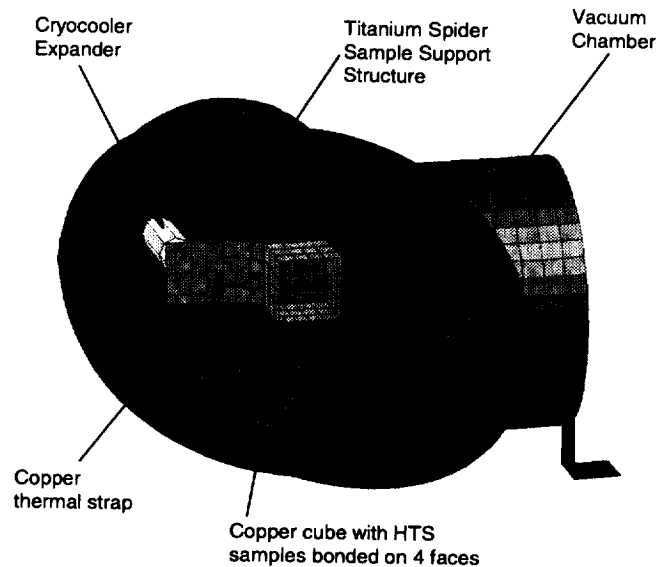


Figure 9. Interior view of structural vacuum chamber model.

Of the six separate analysis tasks previously identified, the full experiment finite element model shown above was used for the first two tasks, the complete stress and modal analyses for the experiment. For analysis tasks 3-5, portions of the full experiment finite element model were separately analyzed for the specific local phenomena being investigated. For analysis task 6, a separate, more detailed finite element model of the copper cube, epoxy bonds and boards were developed to look at local thermal expansion issues; this model is shown in Figure 10.

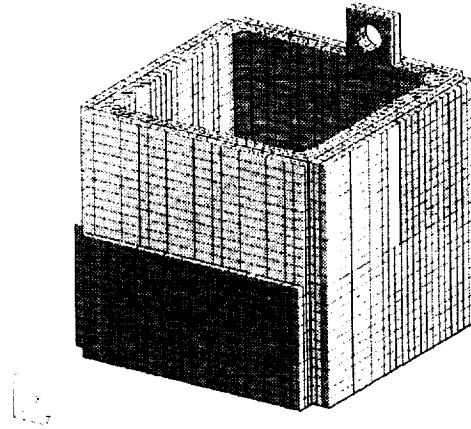


Figure 10. Copper Cube, Epoxy, & Boards Detailed Model

Stress results for primary structure are summarized in Table 7. Von Mises stress (σ_{VM}) as well as margins of safety are shown for all worst-case loads. The load case column refers to the direction of the quasi-static loads (12.5g each axis), where “+++” denotes +12.5X, +12.5Y, +12.5Z, “++-” denotes +12.5X, +12.5Y, -12.5Z, etc. All predicted margins of safety for the various components and fasteners were positive. The lowest margin predicted for primary structure was 0.91 on an electronics box mounting bracket at a baseplate fastener location. The lowest fastener margin of safety was 0.49 on a #1/4-20 fastener attaching the vacuum chamber to the experiment baseplate.

The first mode of the experiment was predicted to be 83 Hz, a “rigid body” mode of the experiment bouncing inside the isolation foam, which was well above the 30Hz requirement from shuttle. The third predicted mode at 92 Hz, a baseplate bending/experiment translation in foam mode, is more visually interesting, and is shown in Figure 11. Unfortunately, the analytical frequency predictions could not be verified by the vibration testing program. The vibration test utilized a middeck locker simulator made of particle board and metal, and the isolation foam, which had several cut-outs for test instrumentation, was not tightly packed into the container. These differences caused the test set up to be more flexible than the actual MIDAS installation in a flight middeck locker, causing the measured frequencies to be somewhat lower than predicted and expected values.

The vacuum chamber submodel and the titanium spider submodel were broken out of the full experiment finite element model and used to assess buckling characteristics on these two assemblies for tasks 3 and 4. Buckling on the vacuum chamber was assessed for an external load of 18.56 psi, simulating a condition where the chamber is perfectly sealed and then experiences maximum Priroda pressure. The analysis predicted buckling at ~700 times this load, indicating that the chamber would fail in yield before buckling. Buckling on the titanium spider was assessed for a 12.5g load applied downward in the axial direction of the spider legs. The analysis predicted buckling failure at 61 times this load, which resulted in a 32 ksi critical buckling stress. Since this stress is well below the yield stress of Ti-6Al-4V, the spider would buckle before it yielded.

Table 7. Primary Structure Margin-of-Safety Summary

Location	Material Allowables		Load Case	σ_{vm} (ksi)	MS _{YLD}	MS _{ULT}
	YLD (ksi)	ULT (ksi)				
Vacuum Chamber	75	115	++ w/18.75 psi external Δp	6.08	8.87	8.46
Vacuum Chamber	75	115	+++ w/4.05 psi internal Δp	6.18	8.71	8.30
Vacuum Cover	75	115	++ w/18.75 psi external Δp	4.89	11.27	10.76
Vacuum Cover	75	115	++ w/4.05 psi internal Δp	4.83	11.42	10.90
Vacuum Chamber Feet	66	76	+++ w/18.75 psi external Δp	12.47	3.23	2.05
Vacuum Chamber Feet	66	76	+++ w/4.05 psi internal Δp	18.52	1.85	1.05
Electronics Box	36	42	+++	10.98	1.62	0.91
Experiment Baseplate	36	42	+++	3.66	6.87	4.74
Experiment Cover	36	42	++	2.75	9.47	6.64
Compressor Support Brackets	36	42	+++	6.60	3.36	2.18
Titanium Spider	120	130	+++	3.02	30.77	20.51
Copper Cube	15	19	+++	0.28	41.86	32.93
Thermal Strap	15	19	+++	3.62	2.31	1.62
*Cryocooler SS Tube	70	85	+++	9.88	4.67	3.30

Required $FS_{YLD} = 1.25$, $FS_{ULT} = 2.0$

* Cryocooler SS Tube is for reference only; precise interior details of tube were unavailable.

The exact internal details of the stainless steel tube connecting the compressor and expander in the Texas Instruments 1-Watt Linear Cooler assembly were unknown. Thus there was uncertainty about whether the mounting of the cryocooler assembly was acceptable since the compressor produces vibrational forces that could cause the assembly to vibrate. Therefore, the tube was assumed to be thin-walled, and the stress in the tube was analyzed under the self-induced vibration mode of the compressor on the mounting stand using a NASTRAN frequency response analysis of the cryocooler assembly. The first phase of the analysis predicted a first mode of the cryocooler subassembly at 304 Hz (compressor rocking axially on the mounting brackets). Since the compressor load was known to be a 0.5-lb load acting at 54Hz, one would expect virtually no dynamic amplification of the compressor load given this modal result. The actual results from the frequency response portion of the analysis predicted a maximum stress in the tube of 2.7 ksi, equivalent to a factor of safety of 26.

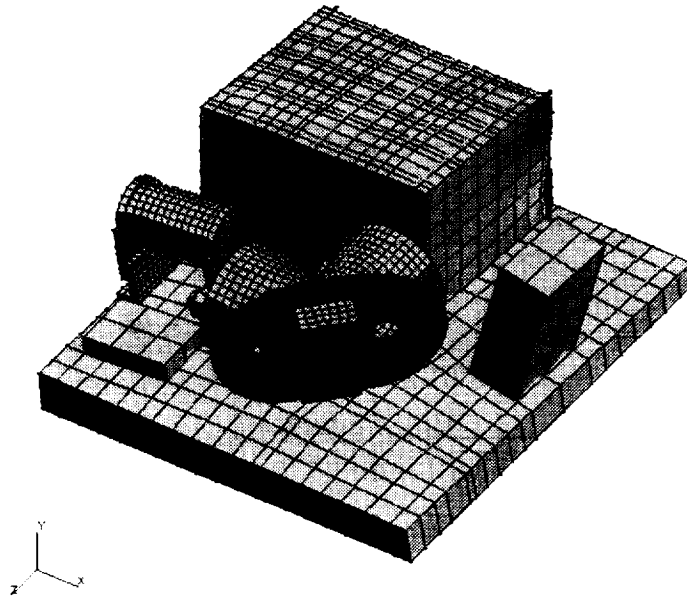


Figure 11. Experiment mode 3: 92 Hz.

The final structural analysis performed was of the copper cube/epoxy/board assembly. While MIDAS was on board Mir, a separate MIDAS experiment running on the ground experienced failures on the bonds and boards during the initial pump down to 77 K. A finite element model, shown previously in Figure 10, was developed of the assembly as manufactured at room temperature. In this model, the cube has exterior 2.5-cm square faces, and the boards are also exactly 2.5 cm square. Analysis showed that when the assembly was cooled to cryogenic temperatures, the copper cube shrunk considerably more than the epoxy and boards, which caused the boards to press against each other and shear the bonds beneath. Based on this analysis and some parallel testing, the ground test cube was resized to be slightly larger than the boards, which provided enough room for the assembly to shrink during the cooling process without causing interferences between the boards.

Modeling assumptions, analysis requirements, and results for all six of the analyses summarized above are described in more detail elsewhere¹⁰.

Thermal Analysis

The challenges in the thermal design and analysis included: thermal isolation methods for the cryogenic samples; design for cooling to cryogenic temperatures; cryogenic epoxy bonds; management of ambient temperature components' self-heating; and fan cooling of the enclosed locker. The cryogenic issues have already been discussed in the design sections. Thermal issues outside the vacuum chamber related to the dissipation of component power. Under normal operation, a total of 55 W had to be removed from the experiment, while maintaining the components within their operating temperature ranges. The maximum allowable temperature of the front panel, as defined by Mir and Shuttle safety documentation, was 49°C^{3,4}. The maximum environmental temperature that could be experienced within Priroda was 40°C, although temperatures actually experienced during flight were normally near 25°C. The heat was

removed using a single fan. Although the experiment was not designed for operation on the Shuttle, the experiment had to be thermally fail-safe to allow acceptable temperatures in the case of inadvertent activation while still on-board the Shuttle in a closed-back locker.

The fan was sized to be able to move at least 65 cfm of air at the lowest supply voltage that could be experienced on Mir. The front panel opening size was set by the fan size. Screens were required because of the possibility of air-borne particulates on Mir, and were chosen for minimum airflow obstruction. A spreadsheet was used to determine the optimum outlet area for the rear panel exhaust ports. The calculation produces the curve of air flow rate versus outlet area shown in Figure 12. This curve was used to determine that any total outlet area for fan exhaust above 160 cm² (25 in²) would be acceptable.

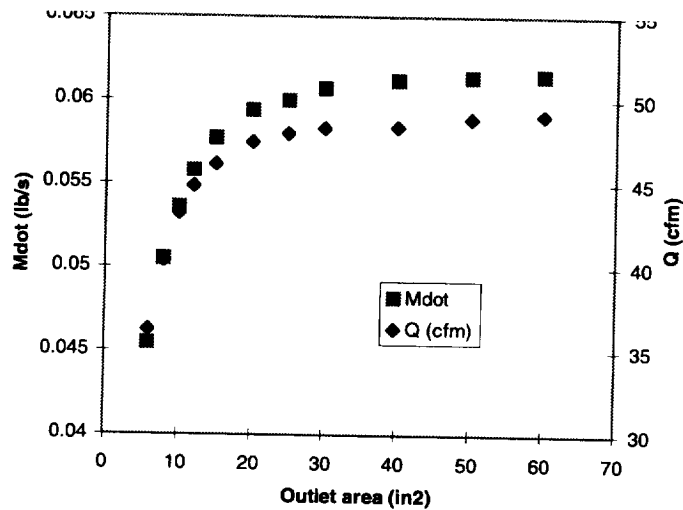


Figure 12. Fan performance versus outlet area.

Thermal modeling of the experiment was done in both PATRAN and SINDA-85. Since the design of the experiment was done in the CAD software Pro/Engineer, parts could easily be imported to PATRAN for meshing and analysis. Also, since the structural analysis was performed using PATRAN models, the models could be shared between the structural and thermal analysts, resulting in substantial increases in efficiency and accuracy. Certain parts were easier to model in PATRAN, as well as allowing easier detailed modeling since Pro/Engineer geometry was available. In general, the modeling in SINDA allows easier transient plotting and quick “what-if” analyses such as changes in MLI effective emissivity, but limits the model to relatively large lumped nodes. The PATRAN models allow detailed evaluation of heat flow, temperature gradient, changes in materials and overall thermal visualization. The P/Thermal analysis engine was used in all runs of the PATRAN models.

Models were developed of the vacuum chamber and cryocooler expander, electronics box, copper cube with boards and active electronics, redesigned flight support stand, and also the entire experiment. The vacuum chamber model allowed a detailed look at the heating around the cryocooler expander and determination of the final cooling fin configuration on the expander. The electronics box model allowed the heating of the individual chips to be evaluated, especially the 486 microprocessor chip. The detailed model of the cube with the boards and active electronics was used to evaluate whether the active electronic parts would induce unacceptable

gradients on the HTS boards, which they did not. A model of the redesigned flight support stand with the cube and coldfinger mount was created to rapidly evaluate the design of the titanium alloy stand for cryogenic use. The gradient predictions for the thermal strap and cube were validated in ground testing and flight. The model of the entire experiment showed that the self-heating of the components was fairly well-controlled, and none were predicted to exceed their maximum operating temperatures, even using worst-case power assumptions. A thermal map of predicted nominal operation is shown in Figure 13.

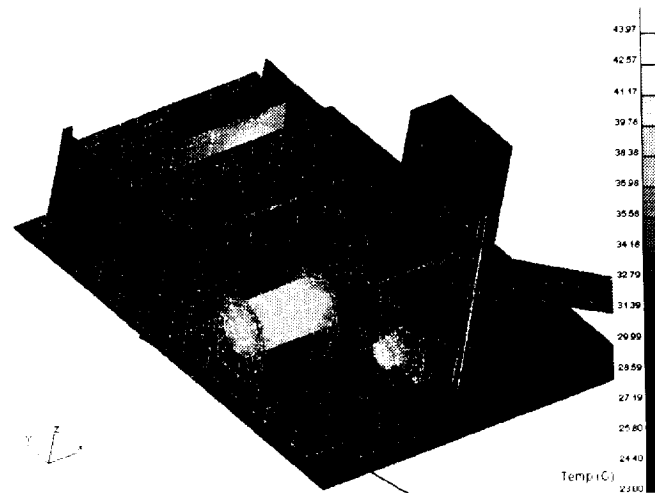


Figure 13. Experiment thermal model prediction.

An example heating distribution during cooldown is shown in Figure 14, with the heat load divided between radiation, wire conduction, and support mount conduction from the ambient environment, as well as heating from the active components on the cryogenic boards. The total heat load absorbed by the cryocooler was predicted to be 410 mW during nominal cooldown and 475 mW in the worst case. Once the cooler reached steady state at 75 K, the measurement frequency decreased and the total load was 330-390 mW depending on conditions. These loads are well within the cooler capacity of 1 W.

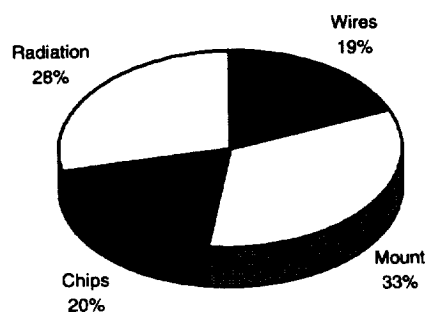


Figure 14. Heat load distribution during cooldown.

In general, the ground testing was a good representation of on-orbit behavior, since cooling used forced airflow and was not dependent on natural convection. The only area for which that did not hold true was within the electronics box. The heating here was mainly from the CPU chip itself, although all components were chosen for their low power output. Since the

electronics box was a closed unit, the interior was dependent on air conduction and contact conduction for removal of heat. On Earth, the transfer of heat from the components to the box exterior would be aided by natural convection, which would not be the case on-orbit. Thus it was desirable to be able to demonstrate a good safety margin in the electronics box temperature during ground testing. Originally, the CPU chip was designed to have a copper strap connecting it to the box exterior, so that its temperature would be kept very close to that of the aluminum box. However, this strap caused electrical grounding problems during ground testing, and was eventually removed from the flight unit.

The model of the experiment's cryogenic portion was compared to the ground testing data, with no post-test correlation or adjustment of the model. This plot of the coldfinger temperature (for prediction versus test) is shown in Figure 15. The analysis predicts the shape of the cooldown very well, and is conservative as it reaches the steady-state condition. The cryocooler successfully cooled the entire sample mass to less than 80 K in less than an hour. The predicted load on the cryocooler was found to be accurate in that the cooler performed as expected during testing.

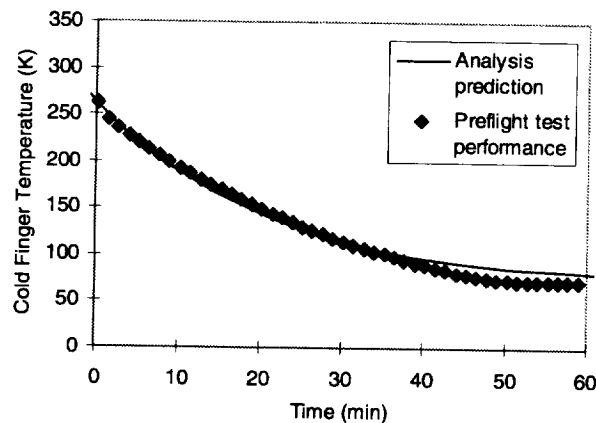


Figure 15. Prediction vs. performance for cooldown.

The thermal models were also compared to the actual performance of the flight experiment in terms of self-heating of ambient temperature components. The four points that could be compared are the locations where housekeeping temperature sensors were mounted – the CPU chip, cryocooler compressor, cryocooler expander and vacuum chamber. The models predicted the tested thermal behavior within 5°C in most cases, both in terms of steady-state temperatures and transient curves. The only exception was the CPU chip temperature prediction, which was too low by 15°C. This could be a result of insufficient detail in the board model to be able to predict a chip temperature, i.e., not including solder joints, detailed trace paths, connector pins, etc.

Assembly

Vacuum chamber assembly

Assembly of the flight vacuum chamber was started on June 7, 1996. The vacuum chamber assembly included the experiment baseplate, since that was necessary to maintain the relative positions of the vacuum chamber and cryocooler compressor. The chamber was first assembled with an ion gauge mounted on the mini-ConFlat flange in place of the ion pump so that the pressure could be monitored during pumpdown. The ion gauge was replaced with the ion pump after successful bakeout and pumpdown were achieved.

Many segments of the vacuum chamber assembly were demanding because of the small size and the sensitivity of the HTS samples to moisture contamination. Exposure to humidity was minimized by bagging the assembly in dry nitrogen whenever possible. The 72 wires extending from the hermetic connectors to the cube and coldfinger were 36 gauge, which meant they were not only fragile but also difficult to see. The bottom MLI blanket had to be wrapped completely around the cube and thermal strap, and penetrations were cut in the blanket for the sensor wires on the coldfinger. The sensor wires were extremely fragile, and not visible from above the cube without the use of a specialized mirror. At every stage of assembly, the performance of the HTS specimens and sensors was verified by measurements at the hermetic connectors' outer face, and all assembly was accomplished successfully.

All internal chamber parts were thoroughly cleaned and vacuum baked before assembly, to remove as many contaminants as possible. Although a layer of water vapor would reabsorb on the parts during assembly, it was still felt that vacuum baking was valuable for the removal of any other contaminants. All parts that were to be installed within the chamber, such as the MLI blanket, connectors, support stand and bolts, were also cleaned and vacuum baked. The temperature of vacuum baking that could be performed after assembly was limited by the cryocooler, HTS materials, and adhesives. Final cleaning that could be done on the HTS boards was limited since most solvents would be detrimental to the superconductive materials.

Vacuum chamber pumpdown

Many difficulties were encountered during pumpdown of both the engineering model and flight vacuum chambers. The engineering model chamber was baked extensively and kept under vacuum by a combined cryopump/turbopump system for six weeks. Nevertheless, the ion pump still had difficulty maintaining the pressure level within the chamber when it was valved off. A calculation of all the loads was performed¹¹ with the results shown in Figure 16. It was determined that the two largest outgassing offenders were the fiberglass cone used for mechanical support of the cube, and the large, two-piece MLI blanket. The predicted MLI load was three times the O-ring load, even though the O-ring load included both estimated outgassing and leak.

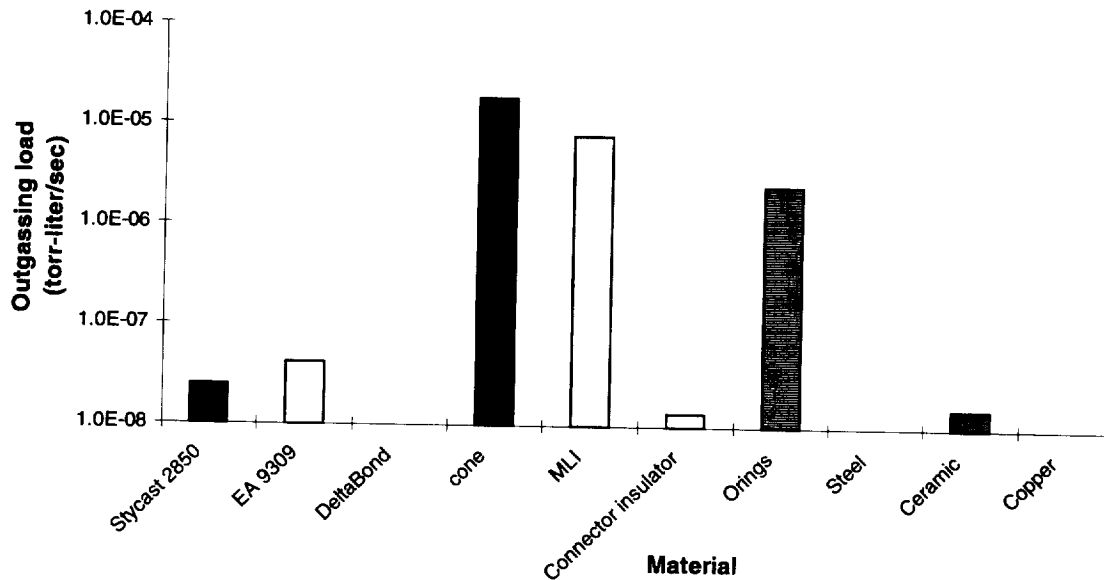


Figure 16. Outgassing loads by material.

After several iterations of vacuum baking, leak checking and troubleshooting (including changing the valve operator on the chamber to a pinch-off tube for sealing), the engineering model chamber was pumped to a vacuum of 6×10^{-6} torr by the main pumping system. At that point, the outgassing rate was checked and found to be 9×10^{-7} torr-liter/sec, and the ion gauge was replaced with the ion pump. The system was continuously flushed with a positive pressure of nitrogen during the changeover of gauge to pump, to minimize the intrusion of water vapor and other contaminants into the system. The system needed to be re-baked afterwards, because the bottled nitrogen used for flushing during the change-out was not completely free of moisture. As a lesson learned from this project, flushing for sensitive systems such as this one is now done using a drying system (i.e., a condensing cold trap) on the gas flush line.

After baking several times at up to 80°C , the ion pump was able to maintain the engineering model chamber at vacuum, with a reading of 4.5 V (2×10^{-6} torr). It was later discovered (during assembly of the flight system), that the large MLI blanket was probably causing substantial impedance to free molecular flow out of the chamber. Thus the pressure within the chamber was higher than expected, and the pumpdown was slower.

A test was performed to evaluate the effect of shutting down the ion pump for a period of five seconds. This was done because during assembly the ion pump would have to be transferred from GSE power to power using the flight wiring harness while actively pumping the sealed chamber, thus incurring a period of about two seconds without power. The ion pump survived the test power loss without incident and maintained vacuum in the chamber after the power interruption.

With the outgassing loads identified on the engineering model, design changes were made for the flight vacuum chamber to decrease the load on the ion pump. The fiberglass support cone was changed to a titanium alloy stand, and the blanket surface area was decreased by a factor of ten, as discussed in the design section. Pumpdown of the flight chamber was

initiated on June 28, 1996. The initial pressure rise rate measured was 3×10^{-5} torr-liter/sec. The goal was to bring this value down to 1×10^{-7} torr-liter/sec, since this was a rate the pump was known to handle, but anything lower than the pump specification of 5×10^{-6} torr-liter/sec was considered acceptable. The system was baked three times at up to 80°C. A higher temperature bakeout could not be used because of potential damage to the cryocooler, HTS samples, and hermetic connectors. After a week of vacuum pumping and intermittent baking, the chamber was at a pressure of 1×10^{-5} torr with an outgassing rate of about 2×10^{-6} torr-liter/sec. At that point the ion pump was installed and after pumping down the system, a test of the cryocooler was performed to allow adjustment of the cooler setpoint to the proper temperature. After that test, the chamber was vacuum baked, with the ion pump running. The system was leak-checked several times and no leaks were found; however, the ion pump was unable to maintain the chamber at vacuum when it was valved off from the main system. When the chamber was valved off, the ion pump monitor voltage would eventually "fold over" (i.e., go above 5 V and then start coming down) and the current would continue to rise.

Altogether, the chamber was opened up ten times in attempts to solve this problem, with pumpdown, leak checks and vacuum baking occurring for each of these attempts. At first the problem appeared to be with the ion pump capability, since no leak could be found on the system. The spare ion pumps were tested, and the best was chosen as a replacement. Also, to drive off water vapor, the system was flushed with argon and the system was repeatedly baked. These attempts were not successful in solving the problem. Later, it appeared that perhaps the pumping system was not pulling the chamber pressure down enough and that there must be some blockage slowing the pumpdown. Several venting holes were cut in the MLI to ensure that it was not blocking the chamber pumpdown. On July 15, even though the ion pump was not reliably holding the chamber at vacuum, EMI test data was absolutely required in order for the payload to be acceptable for launch. The unit was sealed up only for this test, then re-pumped. It was re-opened briefly to check that the main vent hole in the MLI was positioned correctly in line with the pumping tube.

The system was helium leak-checked using a quadrupole mass spectrometer RGA after each attempted fix, both with a directed helium flow and by bagging in helium. Finally, an extremely slow leak was found in the system that was very difficult to isolate. This leak took up to 10 minutes to show up in the RGA signal. Each of the following fixes were made after exhaustive leak checking and evaluation of the vacuum performance indicated that it would be the best solution. Each time the chamber was opened for a fix, the chamber had to be vacuum-baked when it was pumped down since water vapor was re-absorbed on the internal surfaces. These fixes took place over the time period from July 9 to August 24, 1996. Some of the leak checking was done while the system was pumped through a leak detector, and some was done using the RGA when the chamber was pumped by the main system.

Because the leak initially appeared to be around the hermetic connectors, the O-rings in the hermetic connectors were replaced and lightly re-greased. The hermetic connectors were found to have potentially low levels of compression on the O-ring, so the flanges and grooves were re-machined to achieve close to 30% compression. The vacuum chamber cover O-ring was inspected and replaced because of a slight imperfection. The flight vacuum cover was re-machined to correct a slight bowing in the surface. During this machining, the engineering model cover was temporarily placed on the system for pumpdown. After machining, the flight cover

was placed back on the system. The pumping was not improved. However, it was noted that the pumpdown had been much more productive with the engineering model cover in place. There was a small difference between the flight and engineering model covers, in that the engineering model cover incorporated a "bump" protrusion, as shown in Figure 5, to make room for the cube as mounted on the fiberglass cone. This feature was eliminated in the flight cover design. It was determined that that bump was actually providing extra flow-through area for vacuum pumping, which was allowing better pumpdown of the chamber. Fortunately, the engineering model cover had been manufactured with flight quality materials and documentation. Thus, the experiment was assembled and flown using the engineering model cover. Figure 17 is a photograph of the completed hardware after installation of the final cover. After all modifications, the ion pump was running at 4.15 V and holding steady when valved off, so the chamber was pinched off from the pumping system. Due to the tight schedule before launch, only two days of bakeout were possible, instead of the desired minimum of five days.

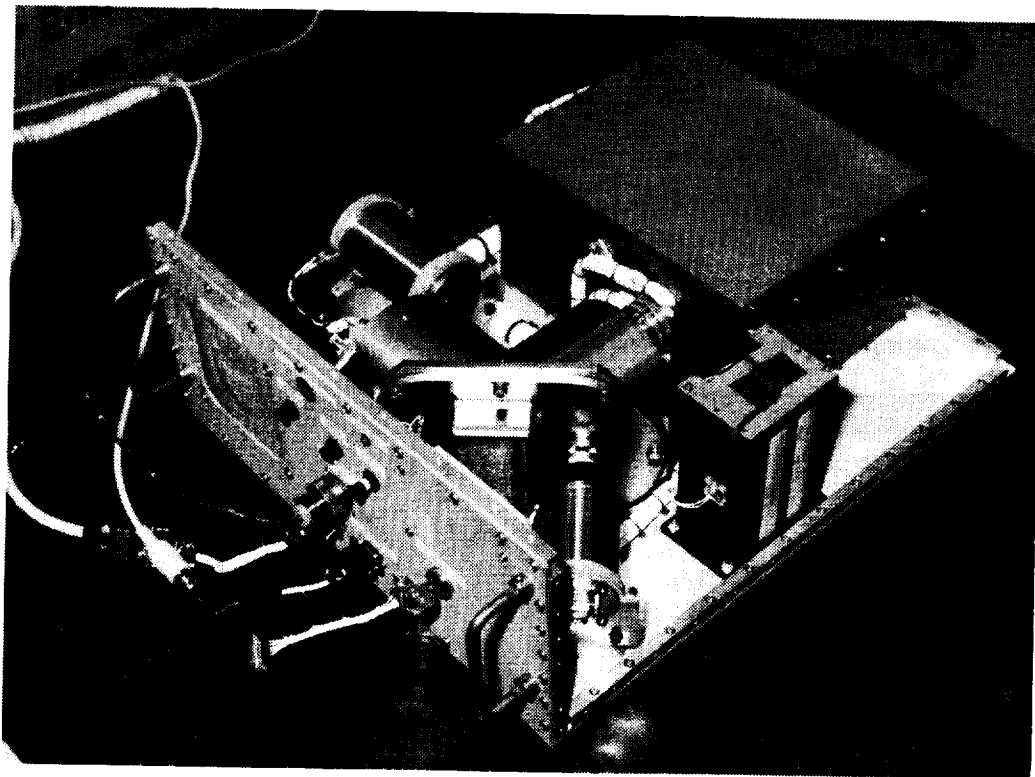


Figure 17. Photograph of flight hardware with final cover, during operation.

Experiment Assembly

Experiment assembly began on June 20, 1996 with the front panel and battery box, parts that did not require the vacuum chamber to be available. When steps were performed that included wiring, all connections were checked as they were made and repaired if necessary. The vacuum chamber was integrated on July 8, 1996. A photograph of the completed hardware is shown in Figure 18, prior to the change of the vacuum chamber cover. The front panel, with key mode switch, connectors, circuit breakers, and labels (in both Russian and English) is shown in Figure 19.

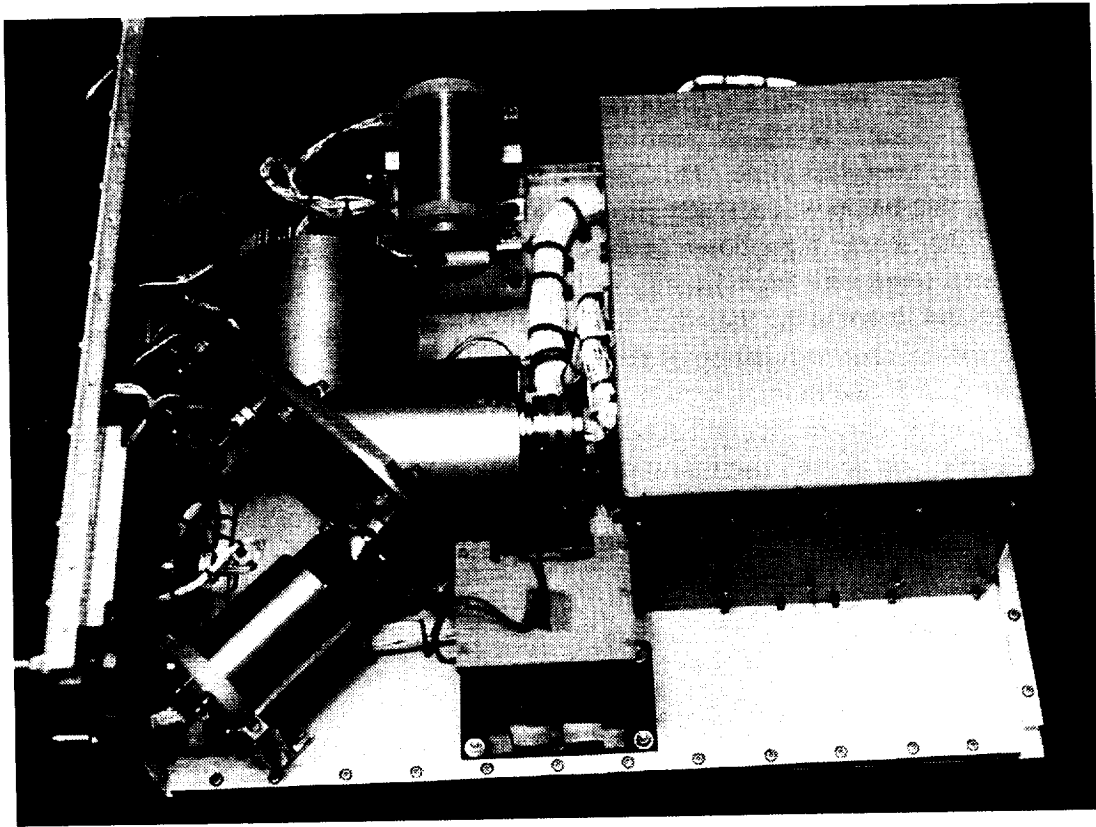


Figure 18. Photograph of interior of assembled experiment.

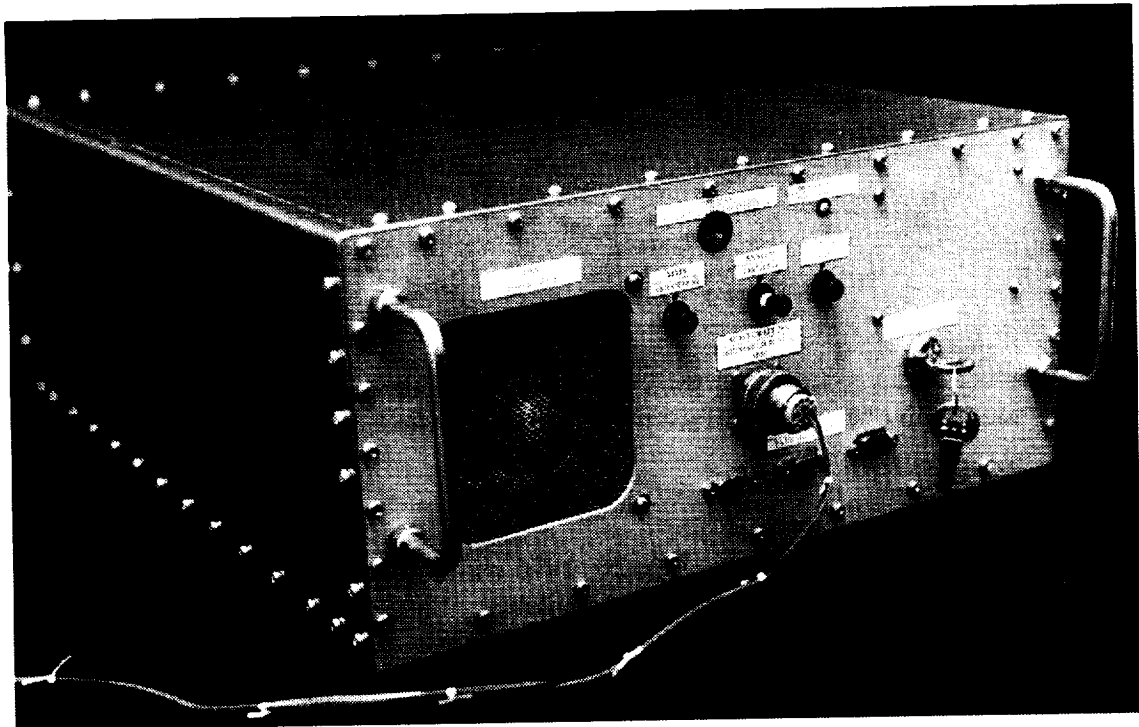


Figure 19. Photograph of assembled flight hardware (view of front panel).

A full functional test was run on August 2 while the experiment was being pumped by the pumping station. This test was a compressed version of the flight operation, where a full flight data set was acquired in a compressed four-day time period by decreasing the timing between measurements. This meant there was more self-heating on the HTS boards than during flight, so the cryocooler used slightly more power, but otherwise this test was a good simulation of flight. The test was fully successful.

The unit was assembled for the final time on August 24, 1996. The ion pump was running at 4.15 V and holding steady when valved off, so the chamber was pinched off from the pumping system. All necessary re-assembly was done. As required for operation on Priroda, all internally exposed surfaces were wiped with hydrogen peroxide to kill bacteria before the cover was put in place.

The unit then underwent thermal and vibration testing. Functional verification was performed as part of those tests, as well as independently for the Russian counterparts who were visiting Langley. Two of the functional tests were performed at 23 and 32V, to span the potential voltage range on Priroda. The electrical tests (resistance, breakdown, startup current and power usage) were also performed for the Russians. With so many functional tests performed in a short space of time, the repeated warmups of the cryocooler constituted a substantial load on the ion pump. The ion pump tended to "fold over" during the warmup of the cryocooler, when many cryopumped gases were released into the chamber simultaneously. After each warmup, the pump would slowly recover, and would fully recover the next time the cooler went to cold temperatures.

All fasteners were staked with Stycast 2850FT epoxy adhesive as the required second mode of restraint (in addition to the fasteners themselves as the first mode of restraint). Staking was performed when a component was mounted and there was deemed to be minimal chance of it being removed. Final staking of the outer case fasteners was not done until just before the last test, which was the vibration test. All connectors were either safety wired or staked. The experiment wiring harness was tied down using cable clamps and Tefzel wire ties to eliminate motion during vibration and handling.

An external 28V battery was used to power the ion pump through the front panel for transport, and the experiment was transported to KSC by van. The final wipe of the exterior with hydrogen peroxide was not done until handover at KSC, so that all handling would be complete.

Testing

All testing required by LaRC, Shuttle and Mir documentation was performed. All tests were performed according to written test procedures that were approved in accordance with the project's configuration management plan. Most testing was performed at LaRC, except for the offgassing testing, which was performed at White Sands, and the pre-launch functional test and center of gravity test, which were performed at KSC.

EMI/EMC Test

The first test performed was the EMI test, because that data was needed immediately for both the Russian and JSC safety personnel. This test was first performed on July 15, 1996 using the engineering model hardware. The test was also performed on the flight unit on August 12, because of a change in the requirements on EMI testing. The EMI test was performed both with only the ion pump operating, for Shuttle requirements, and with the entire experiment operating, for Mir requirements. The test was performed according to MSFC-SPEC-521B. DC bond impedance, conducted emissions and radiated emission were measured. Many spectra were generated during this test, for broadband and narrowband limits, several antenna positions, and Mir/Shuttle conditions. In the transport mode, with only the ion pump powered, all requirements were met easily. With the entire experiment operating, there were a couple of narrow regions in the spectrum where the limits were exceeded slightly, but all were considered acceptable by JSC safety personnel. Two example spectra from the final EMI test are shown in Figure 20. Several problems were encountered and solved during the EMI testing. Initially, power was provided to the experiment using a project-provided power supply, which was plugged into wall power. This was found to add substantially to the EMI noise signal, so the shielded power sources available within the EMI facility were used instead. Also, the original EMI filter designed into the experiment was not adequate, and both the DC-DC power converter and EMI filter were replaced. The location of the EMI filter was moved closer to the input power connector, resulting in acceptably low levels of EMI.

Thermal Test

The thermal test of the flight experiment was performed on August 25 and 26, 1996. Due to the demanding schedule, and since the engineering model unit had undergone eight full thermal cycles with no problems, the thermal test for the flight unit was cut to two cycles. This was considered justified since no components with thermal limits had been changed between the engineering model and flight unit, and thus there should not be direct effects on thermal performance. The operational temperature extremes on Priroda were specified to be 5 to 40°C, although this was a manned "shirtsleeve" environment. Since these specifications already included a wide margin (i.e., flight data showed that Priroda temperatures varied only a few degrees around 25°C), no safety margin was added to these values to create the limits for the thermal test. Transportation and Shuttle (non-operational environments for the payload) survival temperature limits were 0 to 50°C. As shown in Figure 21, the two cycle test consisted of one cycle to operational temperature limits, with operational tests at each dwell, and one cycle to survival temperature limits. In the flight test, the order within the cycles was reversed, and the cold ramp to 5°C was done first. This is not standard procedure (a warm cycle is usually done first and last to eliminate concerns with condensation of contaminants), but since this thermal test was done in dry nitrogen and not in vacuum, this change was not a problem. The reason for doing the cold cycle first was that three full functional tests were to be done close together, and each one placed a sudden large outgassing load on the ion pump as the cooler cryopumped gases from the chamber and then released them on warm-up. The 5°C chamber temperature made it easier for the ion pump to operate, since the vacuum chamber pressure was lower at the lower temperatures. Startup current and power usage testing was done as part of the functional tests to save time. All functional tests were successful.

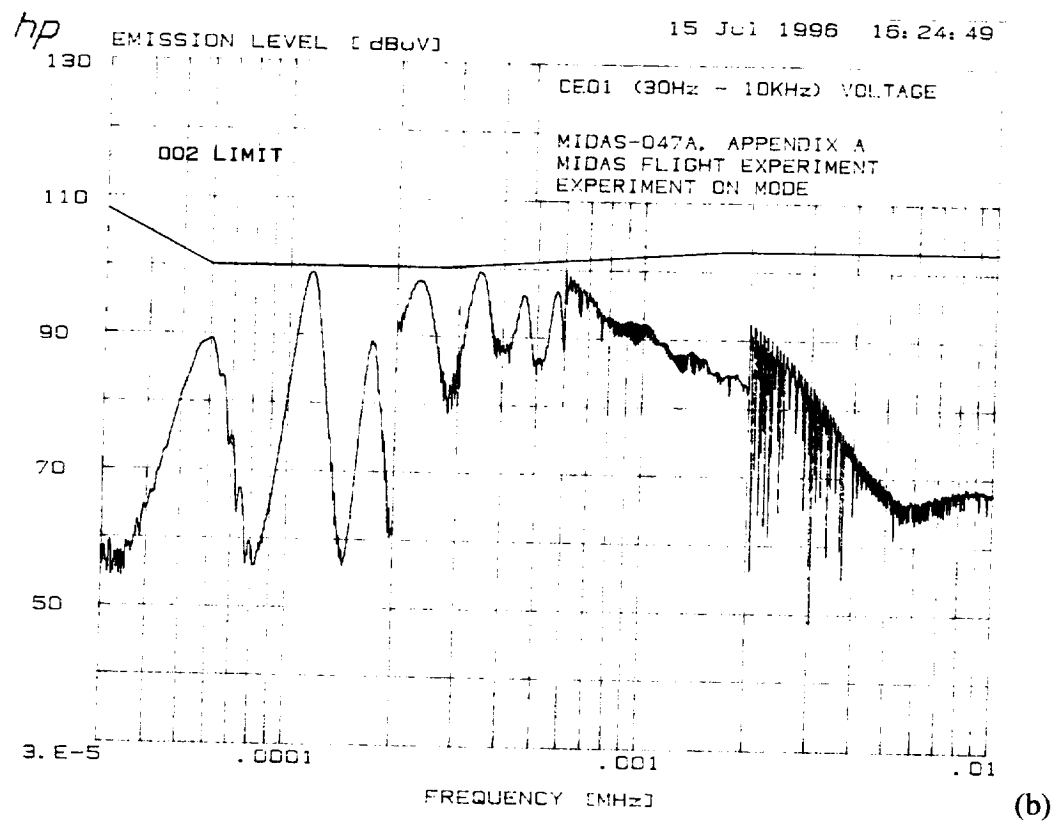
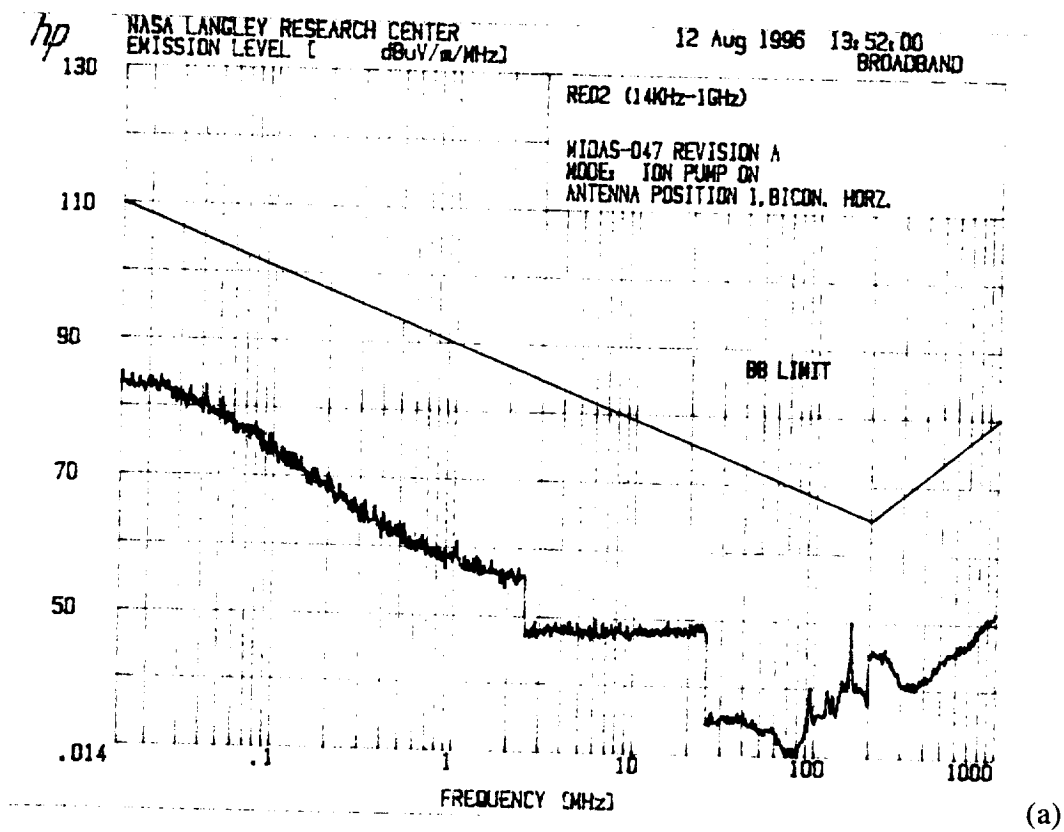


Figure 20. EMI test example spectra: (a) ion pump only, (b) entire experiment on.

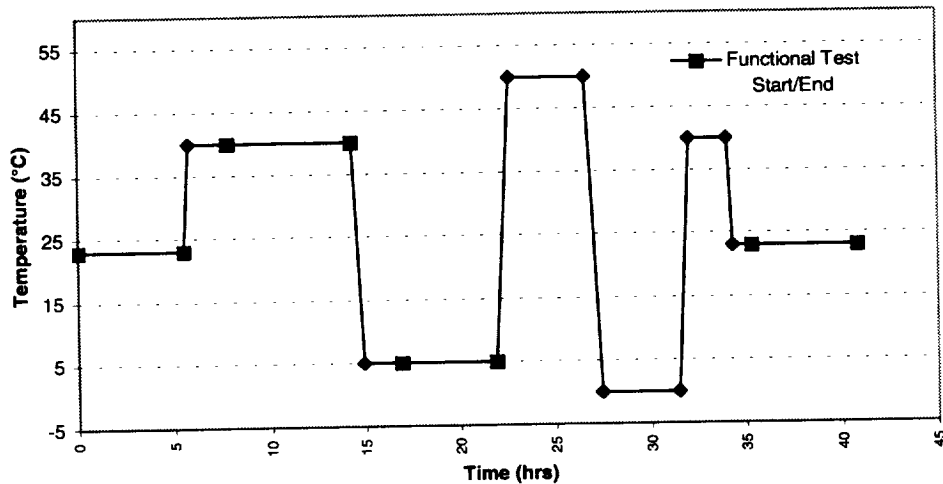


Figure 21. Thermal test cycle.

Vibration Test

The vibration test was performed on August 27. The vibration environment of a Shuttle locker was simulated by mounting the payload in a simulated locker provided by JSC personnel. Layers of foam were applied to the exterior of the case in the same manner as would be done for launch, until the payload fit tightly in the locker. The locker door was closed and the locker was bolted to the shaker table for testing. The vibration spectrum required for Shuttle was used, as shown in Figure 22. Since there were structural changes between the engineering model and the flight unit, the qualification levels of vibration were used on the flight unit as well as on the engineering model (instead of changing to acceptance levels for the flight unit). The payload was subjected to the 9.17 g_{rms} qualification vibration spectrum in three axes for 60 seconds in each axis. A full functional test was done before and after the vibration test (the final thermal functional test was used as the initial test going into vibration). Short functional checks using GSE software were done after each axis of vibration. No problems were observed during or after the vibration test. All functional tests were fully successful.

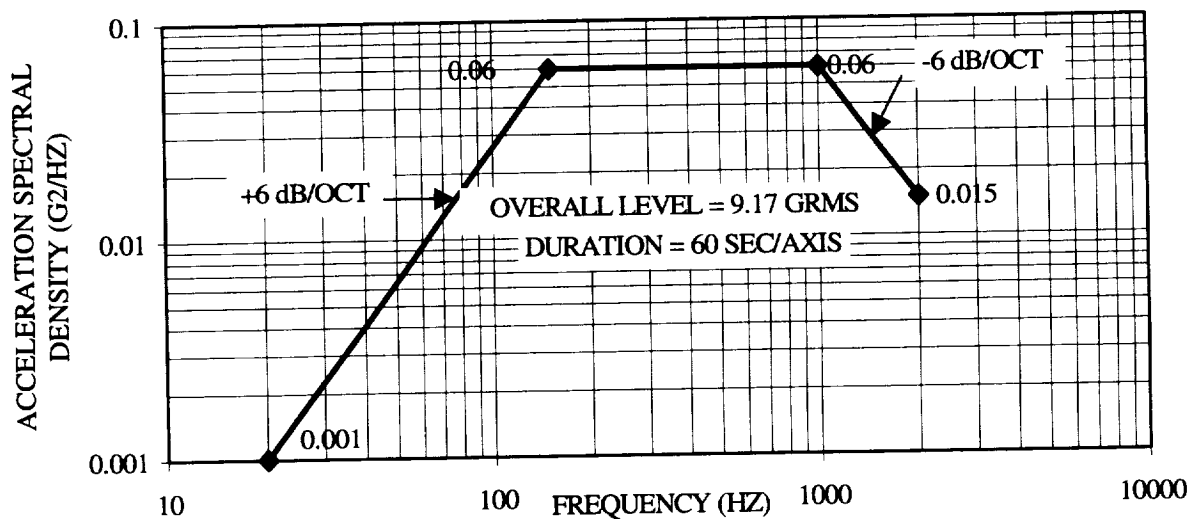


Figure 22. Vibration test spectrum.

Acoustic Test

The acoustic test was performed on the engineering model several times, and since MIDAS was well below the required noise level (60 dB at a distance of 1 meter³), the test was not repeated on the flight unit.

Offgassing Test

An offgassing test is required for all payloads that are to be in manned areas during flight. As a clarification, offgassing is the release of materials in a normal atmospheric pressure environment, as opposed to outgassing, which is the release of materials under vacuum exposure. Offgassing tests are performed to ensure that no hazardous volatiles will be released from the payload during operation or during any temperature encountered. Since the project schedule did not allow for the flight unit to be shipped to White Sands for offgassing testing, it was decided to use a mockup for the testing. This mockup was an experiment case that included all the non-metallic materials on MIDAS in the correct quantities, in approximate locations, under containment conditions more conservative than the flight unit. The mockup was tested at White Sands at 60°C, and met all offgassing specifications.

Other Testing

Three electrical tests were required for operation on Mir. These were Electrical Resistance and Breakdown, Startup Current, and Power Consumption. The latter two tests had to be done over the possible ranges of available voltages on Mir: 23 to 32V. These tests were normally run in conjunction with functional tests that were already being performed, such as during the thermal test.

Also, a four-day software test was run to verify the software operation from start to finish. As mentioned earlier, this test used compressed times for the measurement cycles, so that 90 days of operation could be simulated in four days. To ensure that the flight software times were correct, an additional test was run where the experiment was started in flight mode and allowed to run through one measurement cycle (over one-half hour). Then the times and measurement periods were verified as correct for flight.

While at KSC, the experiment underwent a Center of Gravity (CG) test, which measured the CG at X=11.17 in, Y = 8.18 in, and Z = 4.71 in, where X is along the long side, Y is the width, and Z is the height. The experiment was weighed with the locker and foam; total mass was 29.7 kg (65.5 lb), as shown in Table 1.

Documentation

Logbooks were kept on all flight hardware and most of the engineering model hardware. History of all processes involving the hardware were kept in the logbooks, including assembly, environmental testing and functional testing. Non-conformance reports were written up for all discrepancies. Both the engineer and quality assurance specialist signed off all flight hardware logbooks.

Internal procedures were generated and signed off for all assembly and testing. These procedures were numbered, and are kept both in the MIDAS project files and on the project Web page. The 100-series documents were generated for the interface with Priroda; these were also maintained both in hard copy and on the Web. In addition to the project assembly and test plans, the following documents were also developed: configuration management plan, product assurance plan, system requirements, software requirements, integrated test plan, and software quality assurance plan.

All drawings, CAD files and documents, as well as publications and a list of flight hardware are available electronically on the project Web page (see Additional Sources section). Lessons learned for the MIDAS project have been documented on the project's Web page as well as on the NASA Lessons Learned Information System (LLIS).

Flight

The experiment arrived at KSC on September 4. The experiment was launched on the Shuttle Atlantis (STS-79) on September 16, 1996. Transfer to Mir occurred on September 22, 1996. The experiment operated for 90 days, from September 22 to December 24, 1996.

While aboard the Mir space station, the MIDAS experiment initially cooled the superconductive test circuits to approximately 75K over a six-hour period. However, after fourteen hours, a hardware anomaly occurred in which the ion pump used to maintain the pressure level inside the vacuum chamber became inoperative. Without the ion pump operating, the pressure level in the vacuum chamber began to rise, resulting in a subsequent increase in specimen temperature. The specimens warmed to 95K over a 4-day period and continued to warm to approximately 120K over the remainder of the 28-day cycle. During both the second and third iterations of the measurement cycle, the specimens reached a minimum temperature of approximately 125K, and the temperature remained relatively constant throughout each 28-day period. Although all data were acquired according to the timed measurement schedule, the specimens were only maintained below the superconductive transition temperature for the first few days of the experiment. Figure 23 illustrates the temperature of the cryocooler cold finger during the first and second iterations of the experiment. The temperature of the cryocooler cold finger during the third iteration closely approximates the second iteration shown in Figure 23.

Although the planned minimum temperatures were not maintained throughout the 90-day duration, the superconductive transition temperature and critical current density of each thick film specimen were successfully measured on orbit during the first iteration of the experiment. During this measurement cycle, each of the twelve thick film specimens entered at superconductive state at approximately 87K. Figure 24 shows the resistance versus temperature data for each of the six superconductors on circuits 1 and 3. Circuits 1 and 3 each contain six thick film specimens of the $\text{YBa}_2\text{Cu}_3\text{O}_{7-x}$ superconductor and were fabricated by NASA-Langley Research Center. The abbreviations used in the legends of the graphs indicate the circuit and specimen number associated with each superconductive film. For example, the abbreviation C1S1 refers to Circuit 1 - Specimen 1.

The on-orbit J_c values for the 12 specimens ranged from 1 to 24 A/cm² when measured at approximately 75K. Graphs of the current density versus voltage for the six specimens on

circuits 1 and 3 are shown in Figure 25. The on-orbit T_c and J_c values are comparable to the values obtained for the thick film specimens prior to launch. Figure 26 shows a comparison between the pre-flight and on-orbit data for a typical thick film specimen, indicating excellent agreement in the electrical properties of the films when tested on the ground and in space.

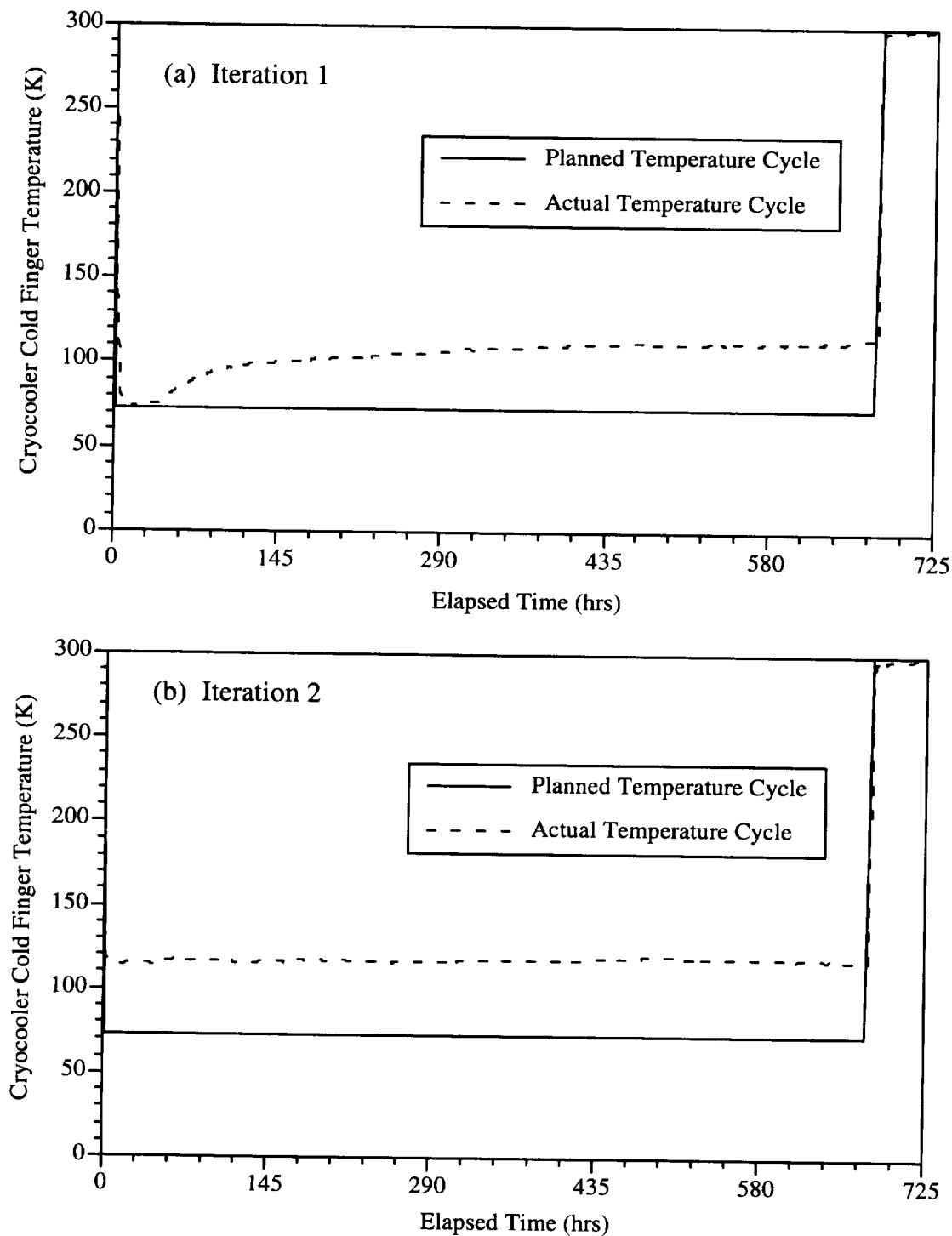


Figure 23. Cryocooler coldfinger temperature during the (a) first and (b) second on-orbit iteration of the MIDAS experiment.

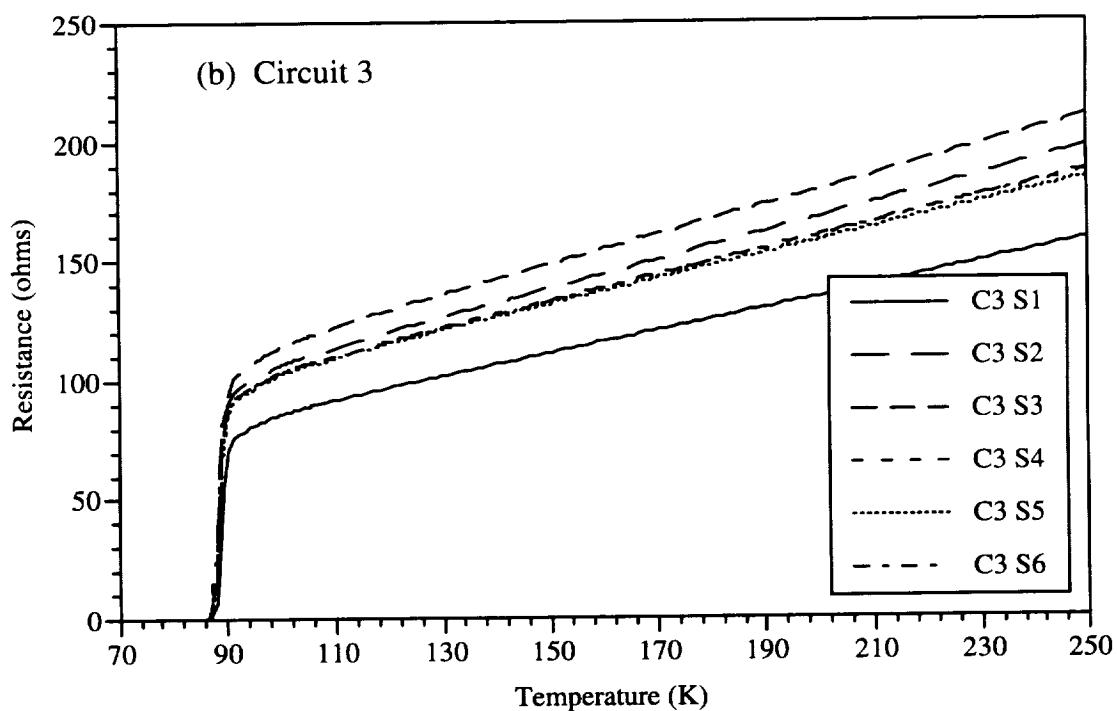
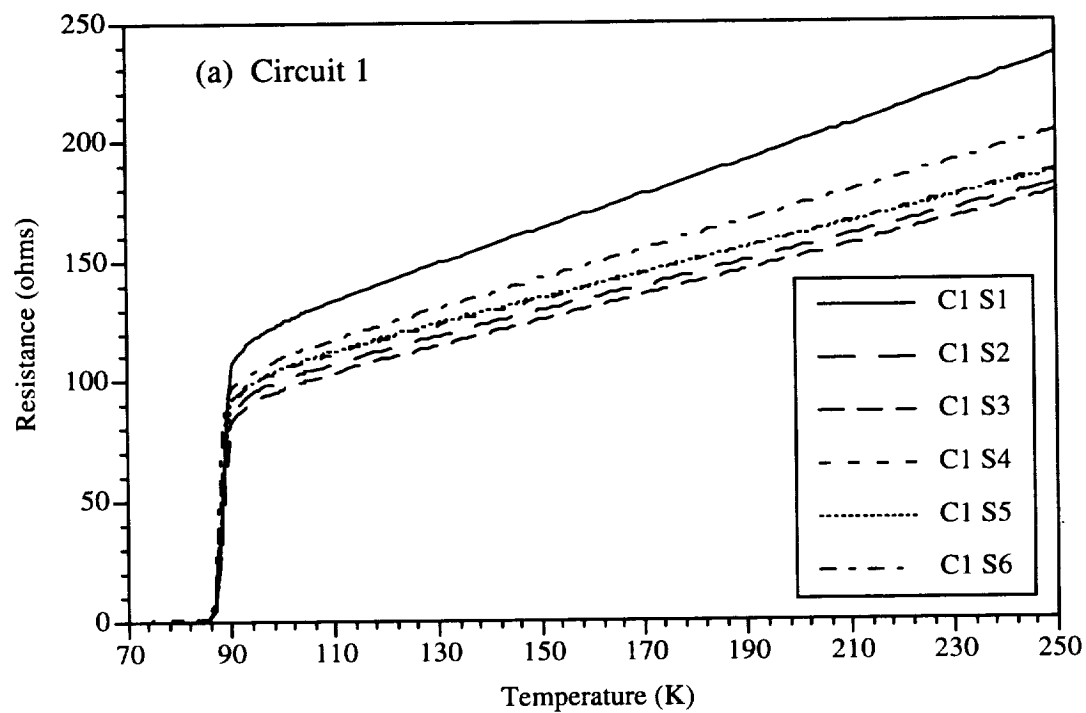


Figure 24. On-orbit resistance versus temperature data for the thick film superconductors on Circuits 1 (a) and 3 (b).

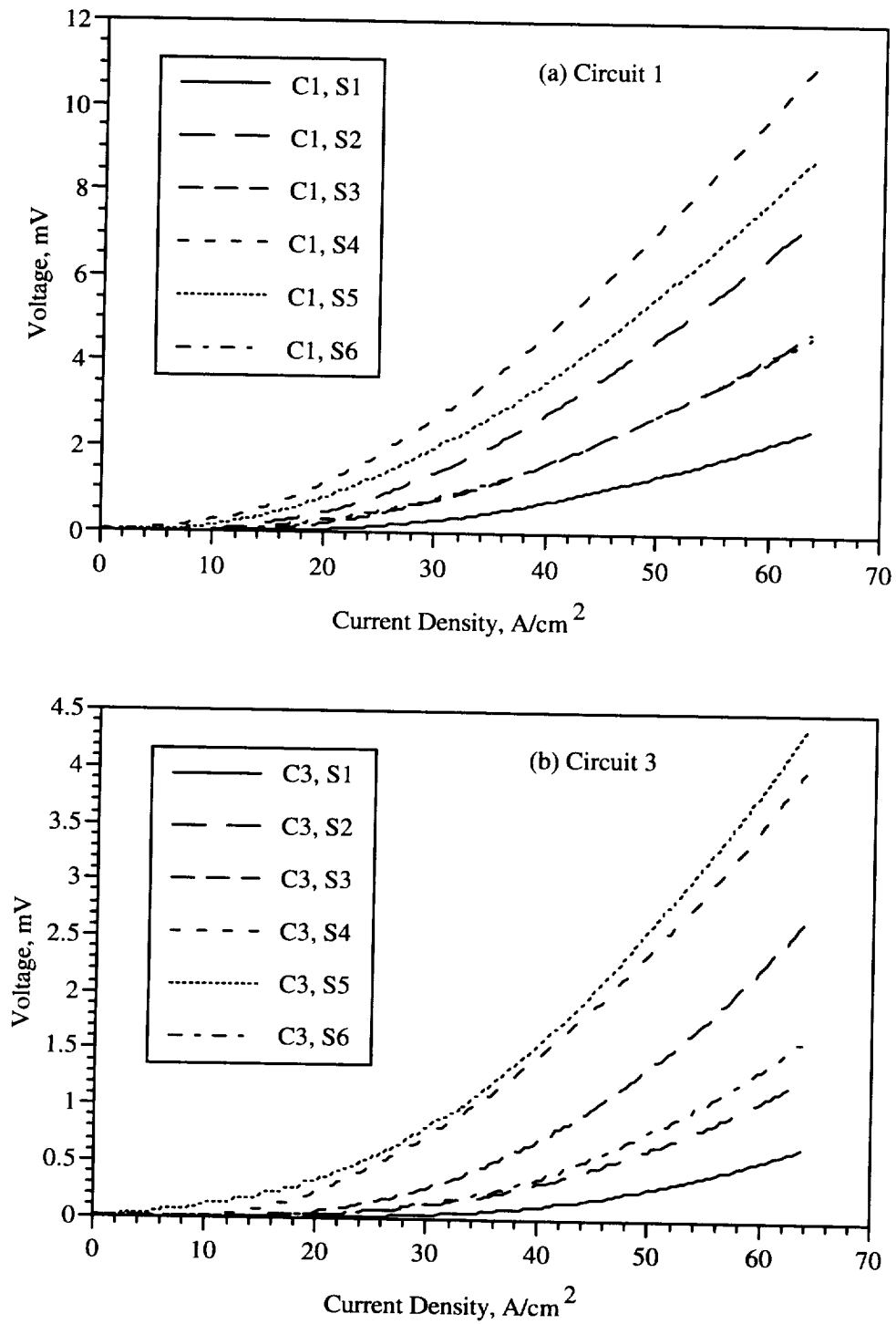


Figure 25. On-orbit current density vs. voltage for specimens on circuits 1 (a) and 3 (b).

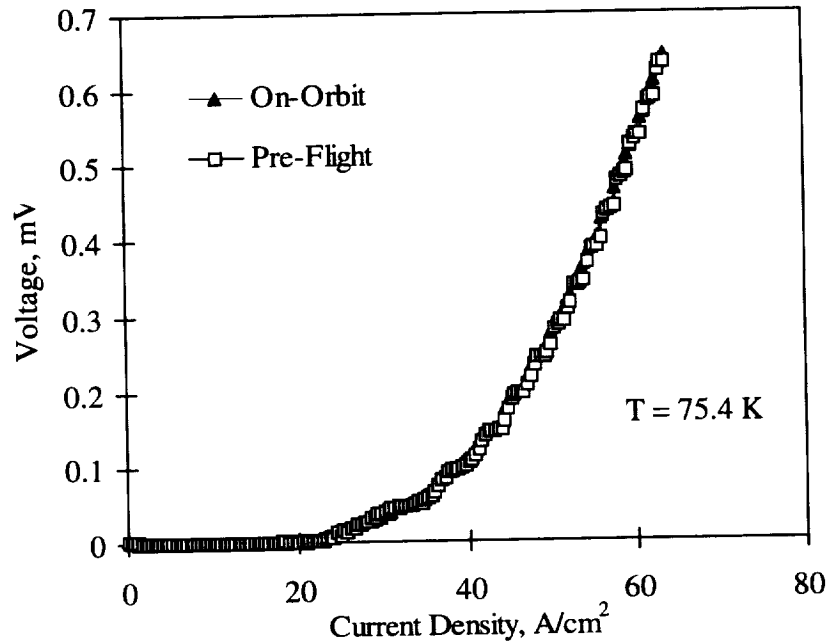


Figure 26. Comparison of pre-flight and on-orbit J_c data for a typical thick film specimen.

During the second and third iterations of the flight experiment, resistance versus temperature data was collected between 120 and 250K. Over this temperature range, the resistance values were found to be equal to those obtained during the first iteration of the experiment. Most notably, the resistance data taken during the final warm-up cycle was identical to that collected during the initial cool-down over the temperature range for which data is available. Additionally, the films exhibited reproducible current versus voltage properties when compared at a constant film temperature of 124K, as illustrated in Figure 27. Additional data from the flight has been reported in the literature^{12,13}.

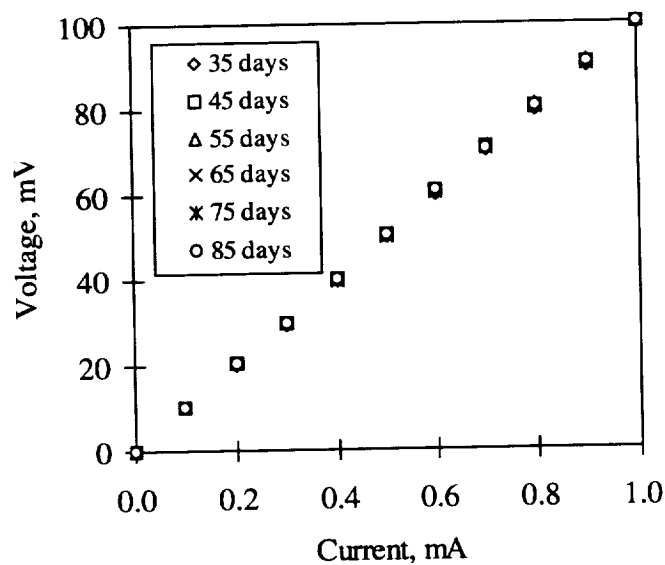


Figure 27. Comparison of on-orbit I-V characteristics at 124K during iterations 2 and 3.

Post-flight Activities

The experiment was returned from Priroda to Earth on STS 81, landing on January 22, 1997. The experiment was returned to LaRC personnel on February 5, 1997, and all flight data was downloaded immediately. It was at this point that the in-flight hardware anomaly of the ion pump failure and subsequent temperature rise was discovered. The experiment was then transported back to LaRC for post-flight evaluation.

Post-flight evaluation of the experiment began on February 13, 1997 when the main experiment cover was removed. One of the first things discovered upon opening the experiment cover was that the propensity of Mir air to contain particulates was not overstated. Regardless of the fact that the experiment interior was absolutely clean when it was assembled, and a fine-meshed screen (which was cleaned periodically on-orbit) covered the air intake, the interior of the experiment had gathered several walnut-sized balls of dust and lint. This situation had been expected since the US/R-002 document³ specifies that Mir may have good-sized particulates in the air. These had caused no verifiable damage to the hardware, although there was a discharge mark indicating that one of the balls of lint might have caused a temporary electrical short.

A series of low-risk electrical tests were performed on the ion pump and on the electronics box to evaluate the condition of the ion pump and the circuitry that controls and records ion pump data. All test results indicated that the ion pump was receiving nominal voltage and the electronics box was recording all ion pump values in a nominal fashion. A check of the backup battery pack indicated that the battery had very little usage during the flight (which was the nominal condition).

Further testing of the MIDAS experiment indicated that the vacuum chamber still had a good hermetic seal and vacuum chamber integrity was not an issue. It was also proven that low supply voltage on Mir was not the primary cause of the previously mentioned flight anomaly. The flight cube (with HTS samples) was removed from the MIDAS experiment and turned over to the principal investigator for evaluation. A “dummy cube” containing only electronics boards (no HTS samples) was installed in the flight vacuum chamber and testing of the MIDAS experiment continued to determine the exact cause of the flight anomalies. No unequivocal conclusion could be reached as to the cause of the problem, but it is probable that the combination of an overloaded ion pump, high temperatures on Mir, and intermittent low voltage were contributing factors.

To further evaluate the superconductive film specimens, testing was also done after spaceflight by performing accelerated measurement cycles. During these tests, a data set roughly the same size as the flight data set was acquired; the measurement time interval was reduced to allow the data set to be collected over a 4-day period. As shown in Table 8, during flight and post-flight testing, each thick film specimen exhibited a superconductive transition temperature ($T_{c,zero}^{\dagger}$) that was within $\pm 0.1K$ of its pre-flight value. Any differences among the values shown in Table 8 are within the temperature measurement accuracy limits of the experiment.

[†] $T_{c, onset}$ refers to the temperature at which the resistivity versus temperature properties of the material just begin to depart from normal to superconductive behavior. This phenomenon is accompanied by a marked change in the slope of the resistivity versus temperature curve. As the temperature continues to decrease, the resistance of the superconductor decreases rapidly until zero resistance is obtained at $T_{c, zero}$.

Table 8. Superconductive Transition Temperatures for $\text{YBa}_2\text{Cu}_3\text{O}_{7-x}$ Thick Films (Pre-Flight, Flight, and Post-Flight)

Specimen	Pre-flight T_c (K)	On-orbit T_c (K)	Post-flight T_c (K)
<u>Circuit 1</u>			
1	87.2	87.2	87.2
2	86.9	86.9	86.9
3	87.1	87.1	87.1
4	86.8	86.9	86.8
5	86.7	86.7	86.8
6	86.9	86.9	87.0
<u>Circuit 3</u>			
1	87.3	87.3	87.3
2	87.1	87.0	87.1
3	86.9	86.9	86.9
4	87.0	86.8	86.9
5	86.8	86.9	86.7
6	87.1	87.1	87.1

Although the $T_{c,zero}$ values of the thick film specimens were found to be unchanged throughout the MIDAS experiment, the post-flight resistance values between 90 and 250K were found to be 1 to 2 percent greater than those observed during all previous tests. A typical example of this behavior is shown in Figure 28. The reason for this slight increase in resistance is unclear considering the last resistance values recorded while on-orbit were in good agreement with all previously acquired data at that temperature. This increase in resistance may be associated with the re-evacuation of the MIDAS vacuum chamber prior to post-flight testing. During this procedure, the vacuum chamber was opened in an argon atmosphere in a glove box to permit the installation of a vacuum valve so that the chamber could be evacuated using an external vacuum system. The installation of this valve was necessary because the system automatically shut down once the 90-day experiment was complete. The ion pump used in the MIDAS experiment was designed only to sustain the vacuum level in the chamber while the system was active and was therefore not capable of evacuating the chamber from the higher pressure that would have developed during the six-week idle period aboard the Mir. Despite the 1 to 2 percent increase in resistance between 90 and 250K, the $T_{c,onset}$ and $T_{c,zero}$ values were not significantly different than the pre-flight observations. Furthermore, the fact that the last resistance values measured on-orbit were identical to the pre-flight values indicates that no degradation to the materials occurred during the 90-day space experiment.

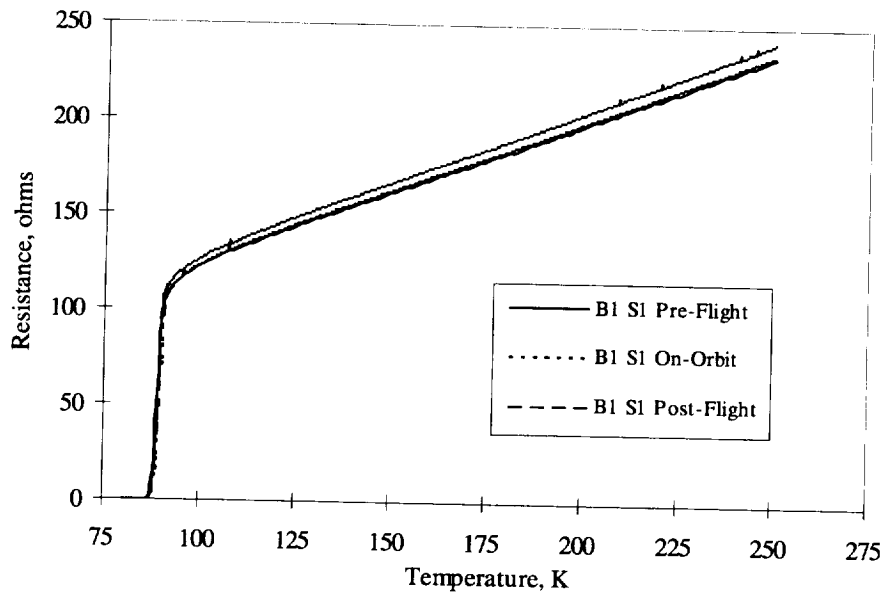


Figure 28. Example of resistance vs. temperature data for pre-flight, flight, and post-flight.

Summary of Development Lessons Learned

MIDAS was an extremely valuable experiment in that there were many “lessons learned” in the development, which can be applied in to future payloads. The following list summarizes some of those experiences.

- Integration of commercial hardware was found to be fairly simple, and resulted in savings of cost and personnel resources.
- The Web page archival was beneficial for MIDAS in terms of communication (internal and with other NASA centers). It was also successful in raising US industry interest in the project and facilitating transition of personnel (since past history is documented).
- The cryogenic bonding of samples was extremely complex. When a bond will be taken to cryogenic temperatures, all possible stress conditions must be evaluated. This includes those caused by a part being at its maximum tolerance for dimension or position, which could cause it to impinge on another part when cooled. Also, the adhesive to be used must be tested under processing and storage conditions that duplicate flight conditions to ensure suitability.
- Soft items such as MLI and wiring bundles that do not seem capable of creating interferences may actually lead to crucial conflicts which are only caught in assembly or testing because they were not shown on assembly drawings. Always indicate wire paths and MLI blankets on top-level assembly drawings and anywhere else appropriate, to help identify potential interference and obstruction problems before assembly starts.
- Everything that is accessible to astronauts or ground crew must have safeties designed in to guard against inadvertent activation.
- The Mir environment has a high number of particulates.

- When designed for EMI ‘cleanliness’, power converters and EMI filters should be matched: bought from the same company and in the same series. When a part is a possible suspect for EMI, always test it separately for EMI as early as possible, rather than waiting for the integrated payload test. This can be an informal test in a local facility, and may not require excessive funding, procedures, or time.
- PC and microprocessor technology is changing so rapidly that when several cards are desired to be exact duplicates, they should be ordered simultaneously and specified as exact duplicates. Specify details such as version of operating system, amount of RAM, RAM mounting configuration, etc. Make sure any batteries on PC cards are included in hazardous materials lists. When using commercial cards, make sure that cadmium-plated bolts are replaced.
- All Shuttle middeck payloads must have the habitable compartment offgassing test performed (many LaRC payloads have had this done at White Sands). It is possible to send a mock-up unit, which only includes non-metallics equivalent to the flight payload but does not have to be operational. Plan the offgassing test early, and determine if a mock-up can be used, or whether a flight-like unit is required.

Many of the lessons learned were related to the vacuum chamber development, and are summarized below.

- Materials to be used in a vacuum must be carefully evaluated. As one example, 3M Kapton tape 5413 looks identical to Kapton tape 1205, and is packaged similarly, but 5413 contains a silicone-based adhesive that is not compatible with vacuum work. The 1205 tape has an acrylic adhesive that can be baked to reduce outgassing.
- For O-rings that must make a vacuum seal, buy them commercially or ensure a good 45° angle is used on the joint, since O-rings with butt joints will probably leak.
- When ordering hermetic connectors, specify that they be shipped with inserts installed. Installing the inserts is a tedious procedure, and can cause damage to the connectors.
- Include ample margin when ordering consumable supplies such as O-rings and copper ConFlat gaskets.
- For vacuum systems, plan the load that will be on the pumping system by calculating all the surface areas of all materials exposed to the chamber, figuring the pressure load due to those materials based on their condition and tabulated values of outgassing (can be found in several references). Add in loads due to leak rates. Then add some safety factor, and any de-rating of the pump necessary for temperature, power available, or aging, before selecting a pump for the chamber.
- When using gas ratios based on a quadrupole mass spectrometer (RGA) to determine if a chamber has a leak (i.e., 5:1 ratio between N₂ and O₂), make sure no pump on the system is pumping one gas preferentially (such as an ion pump or cryopump).
- For moisture-sensitive or high-vacuum systems, use an active drying system for any nitrogen flush, rather than relying on the as-received moisture level in bottled nitrogen.
- Evaluate flow paths in small vacuum systems to ensure efficient and timely pumpdown.

- Make sure the predicted system pressures are well bracketed by the pressure measurement system.
- If a system is baked with the ion pump off, the contaminants driven off of the chamber walls during baking may be driven into the pump, and it will then be difficult to restart. Ion pumps perform best if they are operated as much as possible. If one is not stabilized, run it continuously, especially during any bake of the system. If the system is not baked sufficiently, then turning on a vacuum ion gauge will drive so much water off the walls of the chamber and gauge that the ion pump may not be able to continue running. Vacuum bake the system to remove water (especially if an ion gauge will be used).
- Be conservative in planning time for vacuum bake and leak-checking any flight system.

Conclusions

Although the MIDAS experiment did not fully meet one of the science requirements (for seven days of operational data on the superconductors at or below 80 K), a substantial amount of beneficial scientific data was gathered by the experiment. The fact that the last resistance values measured on-orbit were identical to the pre-flight values indicated that no degradation to the materials occurred during the 90-day space experiment. This was also verified by the comparison of pre-flight and post-flight data. All the T_c curves were recorded during flight, and demonstrated that there was no observable degradation of the superconductors. J_c data was recorded during spaceflight on all sample types, allowing comparisons of samples produced by Russian, Langley, and Eaton co-investigators. Satisfying the secondary objective, a high level of commercial hardware was integrated into the experiment, with associated substantial savings of cost to the program.

Acknowledgments

The work of the entire MIDAS team at NASA Langley Research Center is gratefully acknowledged. The entire project could not be named as authors; in addition to the authors listed, particular thanks go to John Fedors, Robert Dillman, Richard Rawls, Al Porter, Johnny Mau, Walter Wade, Tom Hall, Ralph Stephens, Charles Wittkopp, and Vince Cruz.

Additional Sources

Additional MIDAS information and photographs can be found on the MIDAS WWW home page at <http://amsd-www.larc.nasa.gov/midas/midas.html>.

Symbols

J_c	Critical current density
T_c	Critical transition temperature
σ_{VM}	Von Mises stress

Definitions, Acronyms, Abbreviations

cc	cubic centimeter
----	------------------

CERES	Clouds and the Earth's Radiant Energy System
cfm	cubic feet per minute
CG	Center of Gravity
COTS	Commercial Off-the-Shelf
EMI/EMC	Electromagnetic Interference / Electromagnetic Compatibility
GSE	Ground Support Equipment
GSFC	Goddard Space Flight Center
HTS	High Temperature Superconductors
IBAD	Ion-beam-assisted Deposition
I/O	Input/Output
IPRD	Integrated Payload Requirements Document
JSC	Johnson Space Center
K	Kelvin
KSC	Kennedy Space Center
LaRC	Langley Research Center
LED	Light Emitting Diode
LLIS	Lessons Learned Information System
MIDAS	Materials In Devices As Superconductors
MLI	Multi-layer Insulation
MSFC	Marshall Space Flight Center
OOD	Object Oriented Design
OMT	Object Modeling Technique
OOP	Object Oriented Programming
OOSD	Object Oriented Software Development
PC	Personal Computer
PRT	Platinum Resistance Thermometer
RGA	Residual Gas Analyzer
TBD	To Be Determined
YSZ	Yttria-Stabilized-Zirconia
WWW	World Wide Web

References

- ¹ S. A. Wise, J.D. Buckley, I.G. Nolt, M.W. Hooker, G.H. Haertling, R. Selim, and R. Caton, High T_c Thermal Bridges for Space-Based Cryogenic Infrared Detectors, *Applied Superconductivity* 1 [7-9] pp. 1363-1372 (1993).
- ² M. W. Hooker, S.A. Wise, R. Selim, R. Caton, and A.M. Buoncristiani, High T_c Leads for Remote Sensing Applications. *Cryogenics* 34 [2] pp. 119-122 (1994).
- ³ US/R-002, *Hardware General Design Standards and Test Requirements*. Korolev Rocket & Space Corporation Energia, December 1994.
- ⁴ NSTS 21000-IDD-MDK, *Shuttle/Payload Interface Definition Document for Middeck Accommodation*. NASA Johnson Space Center, March 1988.
- ⁵ M. W. Hooker, S.A. Wise, P. Hopson, N.M.H. Kruse, and J.W. High, Optimization of YBa₂Cu₃O_{7-x} Thick Films on Yttria Stabilized Zirconia Substrates, *IEEE Transactions on Applied Superconductivity*, 5 [2] pp. 1936-1938 (1995)

- ⁶ M. W. Hooker, *Preparation and Properties of High-Tc Bi-Pb-Sr-Ca-Cu-O Thick Film Superconductors on YSZ Substrates*. NASA CR-4761, December 1996.
- ⁷ R. M. Amundsen, *Thermal Design and Analysis for the Cryogenic MIDAS Experiment*. 27th International Conference on Environmental Systems, Lake Tahoe, Nevada, July 14-17, 1997.
- ⁸ MIDAS-045TR, *MIDAS Vibration Test Results*. MIDAS Project Office, NASA Langley Research Center, May 1996.
- ⁹ EHB-2, *SED Bolted Joint Handbook*, NASA Langley Research Center, November 1990.
- ¹⁰ MIDAS-057, *MIDAS Structural Analyses*. MIDAS Project Office, NASA Langley Research Center, June 1996.
- ¹¹ H. G. Patton, "Vacuum System Design Concepts" (class notes), Lawrence Livermore National Lab, p.19, January 1987.
- ¹² M. W. Hooker, *On-Orbit Measurement of the Superconductive Transition Temperatures of YBa₂Cu₃O_{7-x} Thick Films*. NASA-CR-4780, June 1997.
- ¹³ S. A. Wise, *The Effect of Spaceflight on the Critical Current Density of YBa₂Cu₃O_{7-x} Thick Films*. NASA-TM-113130, September 1997.

REPORT DOCUMENTATION PAGE			Form Approved OMB No. 0704-0188	
Public reporting burden for this collection of information is estimated to average 1 hour per response, including the time for reviewing instructions, searching existing data sources, gathering and maintaining the data needed, and completing and reviewing the collection of information. Send comments regarding this burden estimate or any other aspect of this collection of information, including suggestions for reducing this burden, to Washington Headquarters Services, Directorate for Information Operations and Reports, 1215 Jefferson Davis Highway, Suite 1204, Arlington, VA 22202-4302, and to the Office of Management and Budget, Paperwork Reduction Project (0704-0188), Washington, DC 20503.				
1. AGENCY USE ONLY (Leave blank)	2. REPORT DATE May 1998	3. REPORT TYPE AND DATES COVERED Technical Memorandum		
4. TITLE AND SUBTITLE Development of the Materials In Devices As Superconductors (MIDAS) Experiment		5. FUNDING NUMBERS 956-17-00-01		
6. AUTHOR(S) R. M. Amundsen, J. C. Hickman, P. Hopson, Jr., E. H. Kist, Jr., J. M. Marlowe, E. Siman-Tov, C. P. Turner, C. J. Tyler, J. E. Wells, S. A. Wise, R. Dickson, M. W. Hooker				
7. PERFORMING ORGANIZATION NAME(S) AND ADDRESS(ES) NASA Langley Research Center Hampton, VA 23681-2199		8. PERFORMING ORGANIZATION REPORT NUMBER L-17711		
9. SPONSORING/MONITORING AGENCY NAME(S) AND ADDRESS(ES) National Aeronautics and Space Administration Washington, DC 20546-0001		10. SPONSORING/MONITORING AGENCY REPORT NUMBER NASA/TM-1998-208440		
11. SUPPLEMENTARY NOTES Amundsen, Hickman, Hopson, Kist, Marlowe, Siman-Tov, Turner, Tyler, Wells, Wise: Langley Research Center, Hampton, VA; Dickson: Computer Sciences Corporation, Hampton, VA; Hooker: Lockheed Martin Engineering and Sciences, Hampton, VA				
12a. DISTRIBUTION/AVAILABILITY STATEMENT Unclassified-Unlimited Subject Category 16 Distribution: Standard Availability: NASA CASI (301) 621-0390			12b. DISTRIBUTION CODE	
13. ABSTRACT (Maximum 200 words) The Materials In Devices As Superconductors (MIDAS) spaceflight experiment is a NASA payload which launched in September 1996 on the Shuttle Atlantis (STS-79), and was transferred to the Mir Space Station for several months of operation. MIDAS was developed and built at NASA Langley Research Center (LaRC). The primary objective of the experiment was to determine the effects of microgravity and spaceflight on the electrical properties of high-temperature superconductive (HTS) materials. Cooling was provided by a tactical cryocooler, which maintained the specimens at or below 80 K. The superconductive specimens and the coldfinger of the cryocooler were mounted in a vacuum chamber. The entire experiment was mounted for operation in a stowage locker inside Mir. Three separate cycles of the experiment were performed autonomously after circuit breaker activation by the astronaut. Issues discussed include some of the experiment historical background, such as the different spacecraft that were to be the carrier at different times, the selection of components such as the cryocooler and ion pump, and the entire development through design, testing and flight. Some of the many challenges faced by project personnel were maintaining the HTS samples at cryogenic temperatures and in a vacuum, preparation and bonding of the samples, meeting the mass and volume limits imposed by the Shuttle and Mir, and performing all necessary testing to meet required performance standards.				
14. SUBJECT TERMS high temperature superconductors, HTS, space flight experiment, Mir, STS, payload development, commercial			15. NUMBER OF PAGES 60	
			16. PRICE CODE A04	
17. SECURITY CLASSIFICATION OF REPORT Unclassified	18. SECURITY CLASSIFICATION OF THIS PAGE Unclassified	19. SECURITY CLASSIFICATION OF ABSTRACT Unclassified	20. LIMITATION OF ABSTRACT	